3D bioprinting of articular cartilage: Recent advances and perspectives

Marjorie Dufaud, Lilian Solé, Marie Maumus, Matthieu Simon, Emeline Perrier-Groult, Gilles Subra, Christian Jorgensen, Danièle Noël

Bioprinting 28 (2022) e00253

Contents lists available at ScienceDirect

Bioprinting

journal homepage: www.sciencedirect.com/journal/bioprinting

3D bioprinting of articular cartilage: Recent advances and perspectives

Marjorie Dufaud [a], Lilian Solé [a], Marie Maumus [a,b], Matthieu Simon [a], Emeline Perrier-Groult [a], Gilles Subra [c], Christian Jorgensen [a,d], Danièle Noël [a,d,*]

[a] IRMB, University of Montpellier, INSERM, 34000, Montpellier, France
[b] Bauerfeind France, IRMB, 34000, Montpellier, France
[c] IBMM, University of Montpellier, CNRS, ENSCM, 34000, Montpellier, France
[d] Clinical Immunology and Osteoarticular Disease Therapeutic Unit, Department of Rheumatology, CHU Montpellier, 34000, Montpellier, France

ARTICLE INFO

Keywords:
Regenerative medicine
Tissue engineering
3D bioprinting
Cartilage
Bioink

ABSTRACT

Three-dimensional printing, or additive manufacturing, is an engineering process that has been recently applied to the fabrication of tissue-engineered constructs. In comparison with non-biological printing, 3D bioprinting (3DBP) relies on the layer-by-layer deposition of a bioink, consisting of living cells combined with biomolecules and a biomaterial, generally a hydrogel in its liquid phase, which turns to a solid phase when consolidated. In recent years, cartilage 3DBP has gained interest for clinical applications of cartilage tissue engineering and more fundamentally, for *in vitro* osteochondral tissue modeling. In the present review, we address the different 3D printing methodologies available and discuss their advantages and drawbacks. An insight on the current development of bioinks adapted to the printing technology and to articular cartilage tissue engineering is provided. Current challenges and future perspectives are discussed.

1. Introduction

Hyaline cartilage is a highly specialized tissue allowing the smooth sliding of articular surfaces with a low friction coefficient, while being strong enough to support repeated loads. Cartilage comprises a single mature cell type, the chondrocyte, in an extracellular matrix (ECM) mostly made of collagen (COL), proteoglycans and water [1]. It is a highly anisotropic tissue with varying cellularity, biochemical composition and macromolecular orientation along its depth [2]. The highly complex microarchitecture of ECM is responsible for its mechanical properties. Cartilage is an avascular tissue with poor regenerative capacities and focal defects often progress towards degenerative lesions leading to osteoarthritis. Various strategies for cartilage repair, such as bone marrow stimulation, mosaicplasty, autologous chondrocyte implantation, are used in the clinics but with limited success [3]. The absence of effective curative treatment to regenerate or repair cartilage lesions on the long term has prompted the development of tissue engineering (TE) approaches with the ultimate goal of repairing defects with a newly formed cartilage.

Three-dimensional printing, also referred to as additive manufacturing, is an engineering process that has been invented in 1984 to create objects by layering raw materials. These objects are computationally designed in a procedure called Computer Aided Design (CAD). 3D printing has recently been applied to the TE field, and different techniques have been used. One of these is electrospinning in which a polymer filament is elongated under the form of very thin fibers ranging from 10 nm to 100 μm depending on the set-up parameters to build specific patterns [4]. It has been used in cartilage TE to generate biomimicking 3D scaffolds with specific fiber orientations and gradients along the scaffold depth using various biomaterials (for review, see Ref. [5]). However, this technique cannot be used for the 3D bioprinting (3DBP) of living tissues and is out of the scope of the present review. 3DBP can be defined as a process in which cells are mixed with bioactive molecules and a carrier material, generally a hydrogel in its liquid phase, which turns to a solid/gel phase when consolidated. This mixture is referred to as a bioink that allows building of constructs in a layer-by-layer fashion [6]. Since 3DBP enables the design of 3D organized constructs, it appears as an efficient technique to engineer anisotropic constructs such as native hyaline cartilage.

For cartilage 3DBP, bioinks can incorporate differentiated mature cells, such as chondrocytes, or undifferentiated stem cells, such as mesenchymal stromal cells (MSCs) isolated from different tissue sources or induced Pluripotent Stem (iPS) cells. The ideal bioink must have both a biological role in guiding cells towards/maintaining the right

* Corresponding author. Inserm U1183, IRMB, Hôpital Saint-Eloi, 80 avenue Augustin Fliche, 34000, Montpellier, cedex 5, France.
E-mail address: daniele.noel@inserm.fr (D. Noël).

https://doi.org/10.1016/j.bprint.2022.e00253
Received 7 June 2022; Received in revised form 18 October 2022; Accepted 28 October 2022
Available online 11 November 2022

chondrocyte phenotype, and a mechanical role of supporting cells during and after the printing process. By convention, we will name the cellularized objects, "constructs", and the acellularized ones, "scaffolds". Although many reviews have been published on 3DBP, few of them focused specifically on cartilage engineering. In the present review, we aimed at describing the different 3DBP techniques available and discussing their advantages and limitations for cartilage TE. We therefore focus on articular cartilage 3DBP, as opposed to scaffold printing followed by cell seeding, and a detailed review of the literature is provided from rheology requirements to the most innovative approaches.

2. Articular cartilage structure and rheology

Articular cartilage presents a zonal structure comprising of (i) a superficial zone (10–20% of depth) in contact with the synovial fluid, with flattened cells orientated in the direction of shear stress within a densely packed type II collagen (COLII) fibril network, (ii) a middle zone (40–60%) with rounded cells in a randomly arranged collagen fiber network, which ensures the transition between the superficial and deep zones, (iii) a deep zone with ellipsoid cells in a radially oriented collagen fiber network and (iv) a calcified zone with cells trapped in a calcified matrix. Within this whole structure, water and COL contents decrease through the depth of cartilage while proteoglycan content increases from the superficial to the middle zone before decreasing again in the deep zone.

Rheological description of scaffolds and biomaterials is mandatory to optimize 3DBP of cartilage. The mechanical properties of 3DBP constructs should ideally match those of native cartilage. Cartilage is made of a solid ECM phase and a liquid phase. The solid phase is mostly made of collagen (50%–75% of dry weight), predominantly COLII, forming a connected network responsible for cartilage structure and strength [7]. Glycosaminoglycans (GAGs) account for 20–30% of dry weight and are mainly composed of Hyaluronic Acid (HA), but also Chondroitin Sulfate and other proteoglycans, which participate in the mechanical and biological properties of ECM [8]. GAGs are highly hydrophilic and retain a large volume of water, which accounts for 60–80% of cartilage weight. They play a critical role in nutrient and oxygen renewal as well as cellular signalization [9].

The force of the cartilage acting against the applied strain results both from the visco-porosity and elasticity of the tissue. **Elasticity** describes the behavior of a solid, instantly deformed by an external force, then turning back to its original shape when the force stops. The *storage modulus*, abbreviated G′, represents the energy stored by the solid and is used to describe the elastic behavior of the tissue. **Permeability** of the solid phase defines the behavior of the liquid phase that leaks out under mechanical stress and is slowed by the size and tortuosity of the tissue pores. The *loss modulus*, abbreviated G″, describes the dissipated lost energy during one cyclic load and is used to describe the viscous behavior of cartilage that emanates from the liquid phase. Finally, the **viscoelastic** or **poro-viscoelastic behavior** is defined by the complex *shear modulus* G*, which combines the two above mentioned notions: G* = G'+iG'' (in Pa). From a biomechanical point of view, articular cartilage possesses a "viscoelastic" or "poro-viscoelastic" behavior (for review, see Petitjean, in revision).

The *Young's modulus* E (or *tensile modulus*) measures the **tensile stiffness** of a solid, which is calculated by dividing the tensile/compressive stress by the strain. In the case of cartilage, the Young's modulus varies with the applied stress. It can be measured under tension by stretching a sample between two flat surfaces [10] or under compression, it is then called *compression modulus* [11]. Finally, the *shear modulus* G* evaluates the shear strength when the sample is placed between two flat surfaces moving in parallel to each other [12]. Tensile, compressive and shear moduli describe the stiffness of cartilage in the three most common directions, which is around 240–850 kPa for human articular cartilage [13].

It has to be stressed that comparing data from different studies or from different cartilage biopsies remains uneasy – if not impossible – due to three main reasons: (i) the mechanical properties of native cartilage are subjected to inter-individual and inter-joint variations, (ii) the complexity and plurality of mathematical models describing cartilage behaviors (e.g., poro-viscoelastic vs. viscoelastic) and (iii) the multiple experimental settings. Standardization of experimental settings (shear rate, shear speed, strain rate, etc.) or result normalization on healthy native cartilage samples would be needed for proper comparisons.

2.1. Important parameters for optimal 3D bioprinting of cartilage

Efficient chondroinductivity of the bioprinted constructs is essential for successful cartilage TE. In this section, we would like to highlight that chondroinductivity depends on the formulation of bioinks, the crosslinking method, the cell type and the post-printing culture conditions rather than on the bioprinting technique itself. The bioprinting techniques will be described in the next section.

2.2. Diversity of bioinks

Bioinks for cartilage TE can be divided in two main categories: natural and synthetic. **Natural bioinks** are made of biological components and can be carbohydrate-based (e.g., agarose, alginate, chitosan and hyaluronan) or protein-based (e.g., COL, gelatin (Gel), fibrin, silk). Their advantages are biocompatibility, biodegradability and high hydrophilicity with a high swelling ratio to maintain spatial organization [14]. However, in their natural form, they form a physical network stabilized by non-covalent bonds conferring them a weak elastic modulus, which does not reproduce the natural cartilage strength [15]. To alleviate this limitation, chemically crosslinkable hydrogels can be used, most of them being based on UV crosslinking of acrylated derivatives [16]. **Synthetic bioinks** present the advantage to be synthetized in a controlled manner, which allows their chemical, mechanical and biological customization [17,18]. A large number of these hydrogels polymerize forming strong covalent bonds giving them a high elastic modulus, sometimes much higher than the one of native cartilage [18]. However, they are poorly biodegradable and biocompatible. The most commonly used for cartilage TE is polyethylene glycol (PEG) [19–22]. **Thermoplastic biomaterials** can also be mentioned although they do not enter in the bioink category itself since they cannot embed cells. Nevertheless, some of those materials are biocompatible enough to serve as strong supports for cartilage and osteochondral TE. The most common are polycaprolactone (PCL) and poly-alpha-hydroxy esters, in particular polylactic acid (PLA), approved by the federal drug administration for clinical use [23,24]. In addition to the basic biomaterials of bioinks, numerous adjuvants can be added for functionalization. For instance, nanofibrillated cellulose (NFC) gives shear-thinning properties to the bioink, β-tricalcium phosphate (β-TCP) particles improve rheological specifications and enhance osteogenesis while poly(lactic-co-glycolic acid) (PLGA) microspheres releasing Transforming Growth Factor β (TGFβ) are used for chondroinduction [25–31].

2.3. Crosslinking methods

Crosslinking methods are often used to consolidate bioprinted constructs, allowing the switch from a printable to a stiffer but non-printable material. There are two main types of crosslinking methods. **Covalent bonds** can be obtained by photopolymerization, which is the most widely used technique that relies on free radical polymerization and Reactive Oxygen Species (ROS) release thanks to the presence of photoinitiators (for review, see Ref. [32]). For instance, addition of methacrylate groups on gelatin, chondroitin sulfate or HA will form GelMA-, CSMA-and HAMA-based hydrogels that can polymerize when exposed to UV light [23,33,34]. Other strong covalent crosslinking methods exist such as click chemistry or enzymatic crosslinking [31,35].

All these methods form stiff and elastic constructs but use highly reactive chemicals with toxic potential for cells. **Non-covalent weak cross-linking** methods lead to physical hydrogels networks. Interactions include hydrogen bond formation (e.g., when decreasing the temperature in the case of gelatin), hydrophobic interactions (e.g., when increasing the temperature in the case of Pluronic), as well as ligand/receptor or electrostatic interactions [36–38]. This last method is the most used as exemplified with alginate and $CaCl_2$, where divalent Ca^{2+} cations, or other divalent cations, can create ionic bonds between alginate molecules (for review, see Ref. [39]).

2.4. Cell type

The choice of the cell type has to take into account the organizational structure and anisotropy of cartilage as well as the yield of isolation and expansion while promoting cartilage-specific ECM production (for review, see Ref. [40]). Chondrocytes from fetal and adult cartilage are widely used for cartilage TE. Fetal chondrocytes can produce large amounts of ECM *in vitro* but are not clinically relevant since they do not form a zonal architecture. Adult chondrocytes tend to dedifferentiate with the loss of ECM protein production, notably COLII and Superficial Zone Protein (SZP), during the expansion step needed for producing cell amounts compatible with clinical use [41]. This results in the loss of zonal structure required for joint function. Moreover, chondrocyte isolation has other drawbacks, including invasive process to recover cartilage biopsies leading to morbidity at the donor site, low yield of cell isolation and a short lifespan once implanted [20,42,43].

MSCs are also widely investigated for cartilage TE. They can be isolated from different tissue sources, and are characterized by a trilineage differentiation potential leading to cartilage, bone and adipose tissue [44]. Bone-marrow MSCs (BM-MSCs) present a high proliferative capacity and possess the higher chondrogenic potential compared to other sources [45]. However, the use of MSCs requires a differentiation step after 3DBP with a potential risk to generate fibrocartilage or hypertrophic cartilage that both exhibit lower and inappropriate mechanical properties once the construct is implanted. Nevertheless, to overcome these limitations, strategies for enhancing the chondrogenic differentiation are investigated [46,47]. Both chondrocytes and MSCs are used in cartilage 3DBP strategies as proofs-of-concept. However, it might be anticipated that the use of MSCs will be generalized for translational applications due to higher accessibility and availability after *in vitro* expansion. The use of MSCs will make feasible to have sufficient numbers of cells with low immunogenicity that can be used in allogenic settings thereby decreasing the cost of production since one batch can be used for several donors.

2.5. Chondroinductivity

Chondroinductivity of a bioink, defined as its capacity to provide a support for the growth of cartilage, is analyzed post-printing notably by evaluating the expression of typical markers of cartilage. The expression of markers specific for mature chondrocytes (Aggrecan (ACAN), COLII, SOX9), fibrochondrocytes (COLI) and hypertrophic chondrocytes (COLX, RUNX2, vascular endothelial growth factor (VEGF)) can be measured [33,48,49]. Production of ECM components can be quantified using biochemical assays for total GAGs and COL content [19,49]. GAG and collagen contents are normalized to the cell number as quantified by proliferation assays. Besides, production of total proteoglycans and COL can be visualized by histochemical staining (e.g., Safranin O, Sirius Red) and specific proteins (COLI, COLII, COLX, ACAN) can be analyzed by specific immunohistochemical tests [25,50].

2.6. Generalities on 3D bioprinting techniques

In the field of cartilage 3DBP, most studies focus either on the development of chondroinductive bioinks, whose rheological parameters dictate the printing technique, or on the printing technique improvement, which dictates the choice of bioinks. Different types of 3DBP technologies, including inkjet printing, extrusion and light-assisted printing, have been developed (Fig. 1). From a mechanical standpoint, the success of printing depends on the combination of technique/biomaterial/settings. As such, there are three major issues to solve: (i) printability, defined by the ease and fidelity of the print, (ii) biocompatibility, defined by cell viability right after printing and overtime, and (iii) chondroinduction, defined by the ability to induce ECM production. Printability depends mostly on the technique requirements and on the rheology of the bioink [51]. Biocompatibility depends on the printing settings, the mechanical stress applied to cells (e.g., extrusion pressure, printing speed) and the biological specifications of the bioink, including polymerization-associated toxicity [27]. It has to be emphasized that cell mortality induced by shear stress during printing is primarily due to the nozzle design, including shape and diameter [52]. Ideally, viability should be tested 24 h after printing since it was demonstrated that no significant recovery process occurs after this period of time [53]. Notably, printing constructs using conical nozzles with diameters $\geq$260 µm allows a viability similar to that of casted bioinks [21,29]. In most published studies, viability ranges from 70% to 95% [19,48,54,55]. Finally, chondroinduction mostly depends on the biological specifications of the bioink [34].

3. Extrusion-based bioprinting

3.1. Principle

Extrusion bioprinting describes the generation of continuous filaments of biomaterial through a thin tip – might it be a nozzle or a needle – that are then deposited onto a support. It is by far the most used 3DBP technique. This might be explained by the fact that most of the commercially available bioprinters are extrusion-based or include extrusion-based printheads. An extrusion-based bioprinter includes (i) a cartridge system containing the bioink, (ii) an extruding mechanism, (iii) a printhead to load the cartridge and (iv) a controller for printing launch from the CAD file. Extrusion pressure can be applied **pneumatically** (air pressure), by a **piston** – allowing higher extrusion pressure for highly viscous bioinks – or using a **screw system**, which allocates the pressure in a more equal way (Fig. 1). The extruder head deposits the bioink onto a support (e.g., culture plate, Petri dish, glass slide) placed on the printbed and the designed shape is printed in the three dimensions (x, y, z) either by moving only the printhead, only the printbed or both.

3.2. Printing settings

Numerous settings impact the printing outcome, especially the triptych printhead/printing speed/extrusion pressure. The **printhead** can adopt different configurations and different cartridge sizes equipped with tips that have an inner diameter ranging from 150 µm to 800 µm with a minimum filament diameter of 100 µm [23,56,57]. However, the minimal filament diameter can be inferior to the tip diameter when playing with the printing speed, i.e., increasing the speed can result in smaller filament diameters. This **printing speed** must be adapted to the bioink formulation: if it is too slow, the bioink can clog the tip; on the contrary if too fast, the bioink filament can break over its course. The printhead, just like the **printbed**, can be thermoregulated in order to optimize the rheology of the bioink and cell viability. The **extrusion pressure**, which generally ranges from 5 to 200 kPa in case of hydrogels, also influences the bioink flow [26,58]. For the same speed and viscosity, the thinner the tip diameter, the higher the extrusion pressure must be [29]. Finally, the ability of the bioink to quickly and strongly solidify in order to maintain a stable printed shape is another key printability factor. Filament deformation, as measured by the filament spreading ratio (width by height), should ideally be 1 [30]. High

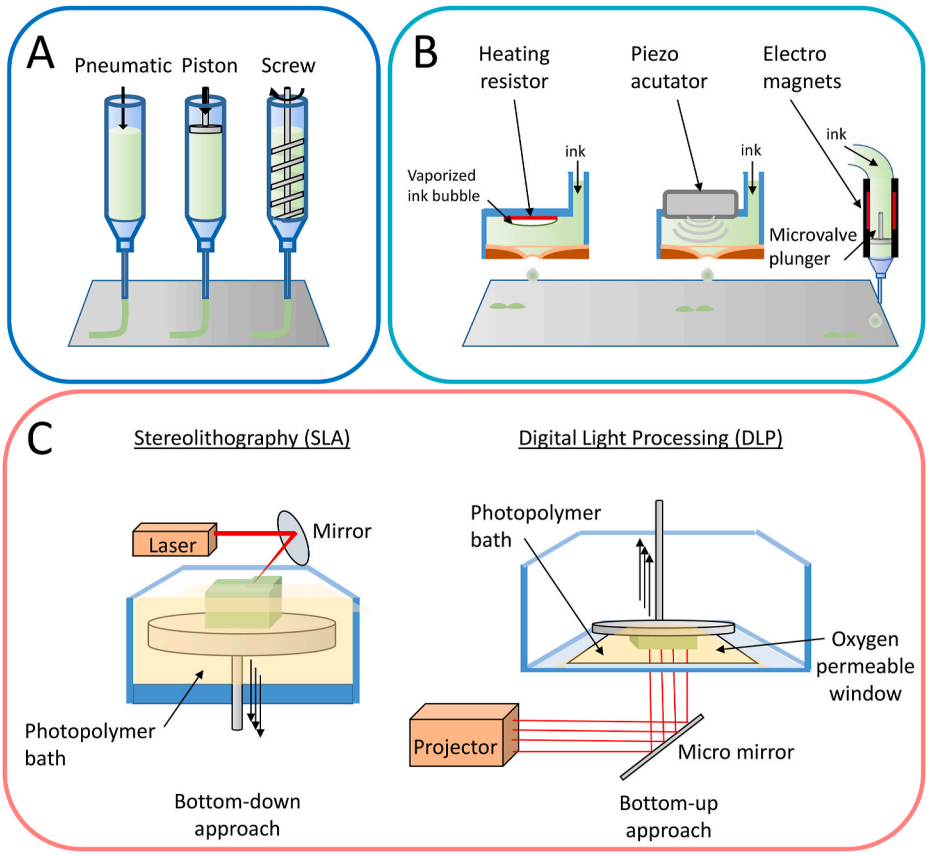

Fig. 1. The different types of 3DBP. (A) Three main types of mechanisms for extrusion printing: mechanical (piston or screw) or pneumatic (air pressure) dispensing systems. (B) Jetting mechanisms used for inkjet printing: heated vaporization, piezoelectric-based vibration or microvalve controlling. (C) Two main types of light-assisted printing: stereolithography (laser) or digital light processing (projector).

viscosity of the bioink allows shape accuracy but requires high extrusion pressure, inducing high cellular stress [51]. A majority of approaches for cartilage 3DBP uses polymerizable bioinks, which can be printed in their fluidic state (G'<G″) and can then solidify (G'>G″) after the polymerization process. Therefore, there is a critical window between printing and polymerization where the printed construct is vulnerable to distortions, impacting its shape fidelity. This is of particular importance for cartilage 3DBP that must generate large 3D constructs to fill and sustain *in vivo* defects of accurate complex geometries.

3.3. Technical improvement

A first strategy aims at improving construct shape fidelity by shortening the time between printing and polymerization. To this end, the most largely used innovation for chemically polymerizable bioinks is the use of a coaxial printhead, which can add the crosslinker during printing [21,26,34,59]. For photopolymerizable bioinks, an option is to have them flowed through a transparent capillary that is exposed to a UV or visible light source allowing simultaneous filament crosslinking and printing [56]. Finally, some thermosensitive bioinks such as gelatin, which is liquid at 37 °C but jellifies under 20 °C, can be printed on a thermoregulated printbed, resulting in an increased viscosity and better shape conservation [60]. Use of shear-thinning materials (e.g., NFC, Gellan gum, Xanthan gum) added to bioinks can benefit from reduced mechanical stress suffered by cells during printing and shape fidelity while they recover their initial viscosity once extruded.

Fused deposition modeling (FDM) printing is a commonly used extrusion-based technique for large construct printing. It consists in printing biocompatible thermoplastic scaffolds (e.g., PCL, PLA) and then print or mold cells-embedding hydrogels within the scaffold, acting as a strong frame for the bioink [21,48,54,61–63]. Thermoplastic biomaterials and bioinks are printed in distinct steps because printing thermoplastic biomaterials requires high temperatures, generally >100 °C. However, the surface temperature of the filament being greatly lower than the melting temperature, it is possible to co-print thermoplastic biomaterials and bioinks with high cell viability (>70 °C) [42].

Freeform reversible embedding hydrogel (FRESH) printing is another extrusion-based technique that allows printing of complex structures from low viscosity bioinks. Using this technique, a cells-embedding alginate bioink was printed using a nozzle immersed in a gelatin bath containing $CaCl_2$, which acted both as a support to build a complex shape and as an alginate crosslinker [64]. Once the construct printed, gelatin could be eluted by heating, which allows to retrieve the polymerized alginate-based construct. In analogous approaches, sacrificial bioinks (e.g., Pluronic) can be designed to support constructs during printing, and then eluted by lowering the temperature, notably to create porous or vascularized-like structures [65,66].

3.4. Advantages and limitations of extrusion-based 3DBP

Extrusion-based 3DBP is the good compromise between cell viability and shape fidelity while it can adapt to a wide variety of bioinks with various viscosities and polymerization processes (UV, thermic, chemical, etc.). The ability to co-print highly viscous bioinks and biocompatible thermoplastic materials makes extrusion-based 3DBP suited for large size constructs with cell densities going up to 1×10^8 cells/mL [67]. Moreover, extrusion bioprinters benefit from constant research, improvement and scale effect cost lowering of FDM, which is by far the most used technique for mass market 3D printing [25,67]. It is the best technology to print well-defined scaffolds with clinically relevant size

within a realistic time frame.

The main drawback of extrusion-based 3DBP is the mechanical stress experienced by cells during printing, which supports that bioink specifications are more restrictive than those used for other techniques. Printing speeds are intermediate compared to other techniques, ranging from 30 to 2400 mm/min, and, with a median resolution of 400 μm, extrusion-based 3DBP is the less accurate printing method compared to the other existing ones [21,23,37,60]. Finally, specialized bioprinter models featuring multiple printheads and clean printing chambers can reach high prices.

3.5. Bioinks applied to extrusion-based 3DBP of cartilage

Gelatin is found among the most used bioink base for cartilage 3DBP using extrusion owing to its thermally reversible gelation particularly suitable to form hydrogels (from liquid at 37 °C to solid below 25 °C). Moreover, gelatin, that arises from collagen denaturation and partial hydrolysis, is translucent and soluble in aqueous solution, and presents a high cell adhesion potential through the conservation of binding peptide sequences present in collagen. In its unmodified form, gelatin is usually mixed with other compounds. Indeed, BM-MSCs loaded within a mix of gelatin, fibrinogen and alginate displayed high cell viability (>90%) and the production of a thick ECM with significant secretion of COLII and GAGs *in vitro* after 28 days [36]. In another study, a composite scaffold made of PCL polymer and a hydrogel of gelatin, fibrinogen, HA mixed with rabbit BM-MSCs and PLGA microparticles encapsulating growth differentiation factor 5 (GDF5) was created [38]. Up to 95% of cells remained viable *in vitro* for 21 days. Implantation of the composite scaffold in full-thickness cartilage defects created in rabbit knees showed a good potential for recreating hyaline cartilage similar in appearance to normal cartilage at week 24. Strong ACAN and COLII staining validated ECM deposition. A hydrogel made of 5–9% gelatin and 1–2% silk fibroin showed good viability of embedded chondrocytes over a period of 14 days, with significant increase of DNA, GAGs and total collagens [37]. Chondrogenic genes (COLII, ACAN, SOX9) increased on day 14, while COLX remained low. In a more recent study from the same group, a photocrosslinkable composite bioink made of Gelatin/silk methacrylate/PEGDA has been optimized to provide the mechanical properties adapted to the maintenance of chondrocyte phenotype with good results even though longer term and *in vivo* data would add stronger conclusions [68]. Of interest, sulfated alginate in a GelMA-based bioprinted cartilage substitute containing MSCs was used for its high affinity with TGFß3 in a so-called “single-stage” strategy [69]. The capacity of the sulfated bioink to deliver TGFß3 in a sustained manner allowed to trigger MSC differentiation towards the chondrogenic lineage and ECM deposition over 21 days.

In its methacrylated form **GelMA**, gelatin has also found its success in bioprinting since it can form a hydrogel that can be (i) easily mixed with cells in physiological conditions in its liquid state, (ii) bioprinted at a temperature close to its gelation point and (iii) quickly consolidated using UV-photopolymerization for long-term *in vitro* culture. Here again, GelMA is rarely used as the sole component. Indeed, a great proportion of GelMA-based bioinks also contain alginate or HA or chondroitin sulfate [23,33,34]. This mix promotes high cell viability, as well as ACAN and COLII induction. When TCP particles were added to the mix, the upregulation of COLX as well as alkaline phosphatase (ALPL) was observed, which can be beneficial to replicate the calcified zone of cartilage [34]. Another common association with GelMA is HAMA. 3DBP of MSCs in GelMA-HAMA constructs allowed chondrogenic differentiation and neocartilage formation *in vitro* after 8 weeks [70]. *In situ* 3DBP of MSCs-laden GelMA/HAMA-based constructs in full-thickness chondral defects created in sheep knee joints resulted in the formation of a neocartilage tissue expressing COLII and proteoglycans [71]. An interesting strategy has been devoted to develop a bioink capable of recruiting MSCs at the cartilage defect site [72]. A GelMA/dECM-based bioink comprising of a 66-based DNA aptamer HM69 that recruits MSCs and supplemented with TGF-ß3 formed a bifunctional bioink system capable of both recruiting MSCs and promote their differentiation. Co-printed with PCL to enhance the mechanical strength of the whole construct, the mix led higher upregulation of chondrogenic markers compared to unfunctionalized or monofunctionalized constructs both *in vitro* and *in vivo*. Importantly, cartilage defects were almost completely filled 6 months after surgery with the formation of a hyaline cartilage-like neotissue and good integration with the native surrounding tissue. Nonetheless, improvement of the neotissue formed, in terms of structure and mechanical properties, still need to be obtained to reproduce the native cartilage structure.

Alginate is also widely used for cartilage TE applications, and notably in bioprinting due to its ability to ionically crosslink with divalent cations such as Ca^{2+}. It is isolated from the cell wall of brown algae and, just like gelatin, it is translucent and presents a high aqueous solubility. Another major key advantage of this material is that it is an Food and Drug Administration (FDA)-approved material for regenerative medicine. Alginate is relatively bioinert and is thus rarely used alone, and when it is the case, it is usually co-printed with a thermoplastic material, such as PLA or PCL, as a reinforcing frame [42,54]. In both cases, high cell viability was maintained. High production of COLII in the ECM was promoted [42]. An association that has shown promising results is a mix of alginate with HA – alginate serving for printability and HA for cell adhesion through its CD44 receptors while maintaining multipotency – co-printed with a PLA frame to resist mechanical stress [48]. This association promotes production of high levels of COLII, ACAN, SOX9 compared to alginate alone while maintaining COLI and COLX levels low or even undetectable.

Alginate is frequently used in combination with nanocellulose isolated from wood fibers for application in cartilage bioprinting [28,29,58,73,74]. Nanocellulose is biocompatible, stable for long periods and presents a shear-thinning behavior particularly adapted to extrusion bioprinting since it ensures cell protection during the printing process. In an effort to move closer to clinics, the behavior of 3D bioprinted cartilage constructs was analyzed *in vivo* over a period of ten months [75]. A commercial bioink of nanocellulose and alginate containing a 20:80 ratio of human chondrocytes and human BM-MSCs or stem cells from the stromal vascular fraction (SVF) was bioprinted. The constructs were implanted on the back of nude Balb/C mice divided into 3 groups: (i) cell-free constructs, (ii) constructs with a mix of chondrocytes/BM-MSCs and (iii) constructs with a mix of chondrocytes/stem cells from SVF. Better stability and mechanical properties of cellularized constructs compared to acellular constructs were observed, with no significant difference in the two cellularized sub-groups. Cartilage-like tissue was formed with no ossification, necrosis or neoplasms detected after ten months. With the objective to better control possible adverse effects associated to the implantation of 3D bioprinted constructs *in vivo*, the possibility to tune the degradation rate of an alginate-based bioink loaded with BM-MSCs was evaluated using partially oxidized alginate [76]. Because the oxidation strongly impaired the viscosity of the mix, gelatin was added to ensure extrudability while preserving cell viability. The results indicated faster degradation rate with higher proportions of oxidized alginate while a 25:75 ratio of alginate:oxidized alginate promoted GAGs and collagen deposition. Another recent study used an alginate-based bioink to promote long-term stability while maintaining good mechanical properties [77]. Other combinations of alginate with native ECM or Pluronic are found [25,30]. Finally, a study evaluated the effect of electromagnetic field frequency on a 3D-printed PCL and chondrocyte-laden alginate construct [78]. A slight increase of SOX9, ACAN and COLII expression was observed after 7 days when using the highest frequency of 45 Hz compared to 7.5 Hz.

Collagen is a structural protein formed by the supramolecular assembly of peptide chains mainly organized in triple helixes. It is essentially extracted from tendons and appears as a good candidate for cartilage 3DBP owing to its irreversible thermal gelation at 37 °C. It

promotes adhesion, growth and signaling of cells forming a fibrous network that resembles their native ECM. High cell viability of bovine chondrocytes as well as increase in GAGs and ECM components have been reported in some studies using COLII- or COLI-based biomaterials [67,79]. COL mixed with alginate has proven to be more efficient to upregulate chondrocyte gene expression than alginate or alginate/agarose hydrogels [80]. More complex osteochondral tissue can be fabricated using a PCL framework filled with MSC-laden BMP-2-containing atelocollagen in the bottom part of the construct and with MSC-laden TGFβ-containing HA in the upper part [61]. Interestingly, high upregulation of chondrogenic genes (ACAN, COLII, SOX9) was detected in the upper cartilage compartment. Upregulation of osteogenic genes (ALPL, COLI, Osterix) was detected in the two compartments, even though at lower levels in the upper cartilage compartment, which suggested hypertrophic differentiation.

Hyaluronic acid is a linear polysaccharide composed of glucuronic acid and N-acetylglucosamine. It provides its viscosity to the synovial fluid and is one of the main components of cartilage, able to stimulate the growth of chondrocytes. HA has the double role of improving printability and cartilage matrix production favoring the formation of hyaline cartilage rather than fibrocartilage. HA-based bioink with tethered TGFβ1 has been shown to yield chondrogenic differentiation of MSCs *in vitro* compared to constructs with non-covalently incorporated TGFβ1 or without TGFβ1 [81]. HA can be biotinylated and combined with streptavidin and alginate to form a double cross-linked hydrogel allowing ASCs to differentiate into chondrocytes [82]. HAMA or HA modified by addition of norbornene have been used alone or co-printed with PCL to stimulate the production of chondrocyte markers and cartilage formation [21,56]. Similar findings have been obtained with thiolated HA combined with acrylated- and allylated-PEGs [83]. Nevertheless, HA is most commonly associated with other components such as GelMA as previously indicated. Oxidized HA has also been combined with glycol chitosan and adipic acid dihydrazide to generate self-healing hydrogels that can be 3D bioprinted by extrusion and can sustain the chondrogenic differentiation of chondroprogenitor cells [84]. In a recent study, Manuka Honey (MH) was added to methacrylated gellan gum (GGMA) to form a composite bioink and promote higher printability and stability of constructs loaded with MSCs [85]. MSCs tended to form aggregates with a greater production of ECM compounds and higher expression of chondrogenic markers. However, the constructs were limited to 4 layers in height to reduce the exposure of cells to UV photocrosslinking necessary to maintain the constructs overtime. A wide variety of bioinks has therefore been developed for extrusion-based 3DBP, which is by far the most used technique for cartilage TE (Table 1; Fig. 2).

A **decellularized ECM** (dECM) of articular cartilage can be used for 3DBP, considering that ECM structure and composition are tissue-specific and retain the components of natural cartilage (COLII,

Table 1
Types of bioink used in extrusion-based bioprinting for cartilage tissue engineering applications.

Bioink base component	Other components	Crosslinking method	Polymer scaffold	Cell source	References
GELATIN	Alginate	Ca^{2+}	/	MSCs	Barcelo, 2022 [76]
	Alginate + Sulfated alginate	UV + Ca^{2+}	/	MSCs	Wang, 2021 [69]
	Alginate + Fibrinogen	Ca^{2+} + thrombin	/	MSCs	Henrionnet, 2020 [36]
	Alginate + CS-AEMA+HAMA+TCP	Ca^{2+} or UV	/	MSCs or Chondrocytes	Costantini, 2016 [33] Kosik-Kozio, 2019 [23] Idaszek, 2019 [34]
	Fibrinogen + HA + Glycerol	Thrombin	PCL	MSCs	Sun, 2019 [38]
	HAMA	UV	/	MSCs	Di Bella, 2017 [71] Onofrillo, 2018 [70]
	Silk fibroin	Self-gelation	/	Chondrocytes	Singh, 2019 [37]
	Silk methacrylate + PEGDA	UV	/	Chondrocytes	Bandyopadhyah, 2021 [68]
	dECM	UV	PCL	MSCs	Yang, 2021 [72] Behan, 2022 [88]
ALGINATE	/	Ca^{2+}+ UV	PLA or PCL	MSCs C20A4 cells Chondrocytes	Izadifar, 2016 [42] Yi, 2016 [78] Baena, 2019 [54] Chu, 2021 [21]
	HA	Ca^{2+}	PLA	Chondrocytes	Antich, 2020 [48]
	ECM	Ca^{2+}	PCL	MSCs	Rathan, 2019 [30]
	Agarose + Collagen	Ca^{2+} + FBS	/	Chondrocytes	Yang, 2018 [80]
	Pluronic F127	Ca^{2+} or Low temperature	/	MSCs	Armstrong, 2016 [25]
	Nanocellulose Chondroitin sulfate	Ca^{2+}	/	MSCs Chondrocytes or iPSCs	Möller, 2017 [28] Müller, 2017 [29]
	Dermatan sulfate				Nguyen, 2017 [73] Gatenholm, 2021 [58] Lafuente-Merchan, 2022 [74]
	Nanocellulose	Ca^{2+}	/	Chondrocytes + MSCs	Apelgren, 2021 [75]
COLLAGEN	/	Gelation at 37 °C	/	Chondrocytes	Ren, 2016 [79] Diamantides, 2019 [67]
	BMP2 DAH HA + TGF-ß	Gelation at 37 °C	PCL	MSCs	Shim, 2016 [61]
	dECM granules	Gelation at 37 °C	/	MSCs	Isaeva, 2022 [89]
HYALURONIC ACID	Alginate	Streptavidin + Ca^{2+}	/	MSCs	Nedunchezian, 2021 [82]
	/	Thiol-ene reaction	/	MSCs	Galarraga, 2019 [56]
	Glycol chitosan + Adipic acid dihydrazide	Self-gelation	/	ATDC5	Kim, 2019 [84]
	PEG-acryl + PEG-allyl	Thiol-ene reaction or UV	/	MSCs	Hauptstein, 2022 [81] Hauptstein, 2022 [83]
	PEG + pHPMA-lac	UV	PCL	Chondrocytes	Mouser, 2017 [21]
dECM	Silk fibroin	Physical	/	MSCs	Zhang, 2021 [86]

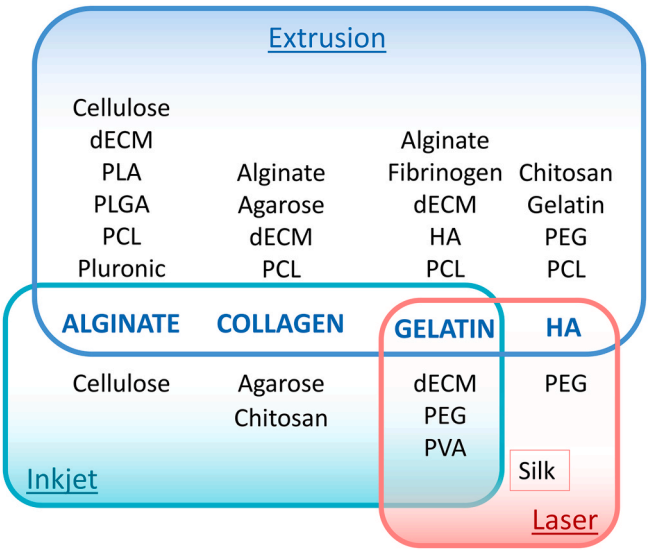

Fig. 2. Main types of bioink used for cartilage 3DBP relative to the printing technology. Alginate, collagen, gelatin and hyaluronic acid (HA) are the foremost base components as indicated in upper case and shared by two or three 3DBP techniques: extrusion, inkjet and laser-based. The additional components that can be mixed to these base components are listed above or below. Bioinks in boxes can be used independently of the base components. dECM: decellularized extracellular matrix, PCL: polycaprolactone, PEG: polyethylene glycol, PLA: polylactic acid, PLGA: poly(lactic-co-glycolic acid), PVA: poly (vinyl) alcohol.

proteoglycans, …) [86]. Thanks to the promotion of cell viability, growth and metabolism, it appears as a promising TE strategy to better mimic this specific tissue. dECM has the advantage of presenting lower immune response risks since those are usually associated to cellular DNA, but great care must be taken in the decellularization process since damage to ECM must be limited to preserve its bioactivity. Decellularization can be obtained by a physical, chemical, enzymatic technique or a combination of them and is considered successful when the remaining amount of DNA is < 50 ng per mg of ECM dry weight and no nuclear material is seen after histological staining [84,87]. The resulting dECM can then be used as a direct scaffold to preserve the native architecture of the tissue or solubilized as (i) a thermally responsive hydrogel for the delivery of cells, drugs and other bioactive molecules or as (ii) cell-laden bioinks. They can be formulated as shear-thinning gels at temperatures below 15 °C before gelation at physiological temperatures preserving the 3D printed shape. It is noteworthy that the rheological behavior of such bioinks is strongly correlated with their protein content, that can itself be linked to the decellularization process [87]. They can be extruded under a filament form to generate 3D structures that can replicate the morphology and function of native articular cartilage. A strategy to optimize the rheological behavior of dECM-based bioinks is to design composite bioinks. A formulation based on 2.5% dECM-5% silk fibroin (w/v) loaded with BM-MSCs allowed to get higher expression of chondrogenic markers compared to silk fibroin bioinks alone, higher protein levels and better *in vivo* differentiation [86]. Methacrylation of cartilage ECM-based bioink promoted chondrogenesis of BM-MSCs as denoted by deposition of GAGs in the construct after a 21-day culture period and increased staining for COLII with increased percentage of ECM in the bioink [88]. In another approach, the use of dECM granules in a collagen-based bioink loaded with MSCs allowed chondrogenesis *in vivo* without addition of any growth factor [89]. Interestingly, the authors showed that even in absence of MSCs, the dECM itself was sufficient to induce neocartilage formation. Nevertheless, dECM-based bioinks generally lack the mechanical properties of native cartilage since the solubilization process that follows decellularization leads to the loss of cartilage structure. The crosslinking of dECM-based bioinks to polymer frameworks may generate constructs that are better adapted to mimic load-bearing tissues [87,90]. Such combinations have notably shown their superiority in promoting human MSC differentiation towards the chondrogenic lineage in comparison to collagen-based constructs.

4. Inkjet 3D bioprinting

4.1. Principle

Inkjet printing, also known as drop-on-demand, is a non-contact printing technology that was the first developed 3D printing method (for review, see Ref. [91]). The procedure precisely deposits droplets of bioink onto a support under control of a dedicated CAD program. The bioink inside the printhead is dropped either by heated vaporization, microvalve control or vibration (Fig. 1). **Heated vaporization** results from the heating of a small volume of bioink at 300 °C during few microseconds within the printhead, resulting in an expanding gas pocket ejecting a drop [19]. The **microvalve-controlled printing technique** allows quick opening and closing of a valve resulting in drop ejection of the over-pressured bioink in the cartridge [92,93]. **Vibration printing** relies on a piezoelectric-based printhead to form a vibration current creating a mechanical pressure that ejects a drop of bioink [94]. The voltage-dependent vibration frequency influences the size of the drop [95].

4.2. Printing settings and technical improvement

Inkjet printing is subjected to superficial tension of the drop that influences the construct shape. Therefore, bioinks with high superficial tension are easier and quicker to eject [96]. CAD settings must take into account drop flattening that occurs following drop propelling at high speeds (e.g., about 8 m/s) and crashing onto the printing support (e.g., a drop of 30 µm in diameter can flatten to reach 18 µm high) [20,97]. To overcome this limitation, an inkjet bioprinter with a resolution similar to existing traditional inkjet printers but with enhanced resolution compared to current inkjet bioprinters has been developed [49]. It allows to eject droplets within oil that prevents cell flattening since oil acts as a structural support during the printing process. Interestingly, this bioprinter also allows to print a number of cells relevant to TE applications, i.e., 3×10^7 cells/mL. The only limitation of this bioprinter up to date is that it can only print two cell types at a time.

4.3. Advantages and limitations of inkjet printing

Inkjet bioprinting is a cost-effective technique because it can be adapted from classic 2D inkjet printers and printheads [98]. It provides high cell viability with an average around 90% [99]. Besides, printing resolution is excellent with precise cell and material deposition within drops smaller than 30 µm, even though resolution depends on the size of the drops and the shape stability of the bioink [19]. Finally, with its high printing speed, inkjet printing is suited for high throughput printing.

The main limitations of inkjet bioprinting are the poor printing quality when using bioinks with viscosities above 3 mPa and when cellularity exceeds a threshold of around 10^7 cells/mL, triggering frequent clogging of the printhead. This greatly reduces the range of compatible bioinks [49]. Notably, using the microvalve-based technique, high viscosity bioinks can be printed but this requires the use of high diameter nozzles that decrease printing resolution and induce shear stress on cells [100]. Regarding piezoelectric-based printheads, the vibration duration (pulse-width) and amplitude (voltage) can impact cell survival and thus needs to be optimized. For instance, a bioink made of agarose and COLI was printed using a 50–350 µs pulse-width and a 40–63 V amplitude in order to obtain single uniform sized drops of 130 µm diameter in a reproducible manner [49]. Finally, thermal inkjet printing uses high temperatures to vaporize the bioink, but this process

is so quick that only cells close to the resistance increase their temperature by 4–10 °C for 2 µs, which is negligible and does not significantly affect cell viability [99]. In addition, thermic printheads are frequently subjected to satellite droplet ejection following the main drop ejection, impairing the printing accuracy [97]. Finally, the low viscosity of printed bioinks makes it harder to print large size constructs when not combined with a supporting frame [65].

4.4. Inkjet-based 3DBP applied to cartilage

Compared to extrusion-based bioprinting, inkjet bioprinting shows less applications in cartilage TE engineering. A set of different base components is used as building blocks of the bioinks: **GelMA** [93], **Alginate/nanocellulose** [51] and **COL/agarose** [49,50] (Table 2; Fig. 2). Other studies have used the synthetic polymer **PEGDMA** alone or mixed with GelMA or acrylated peptides [19,20,98,101,102]. A bioink made of PEG-GelMA allowed the differentiation of BM-MSCs along the chondrocytic lineage [19]. PEGDMA-based bioinks showed excellent cell viability of BM-MSCs after printing and high production of GAGs, SOX9, COLII and proteoglycans was observed when GRGDS peptide and matrix metalloproteinase (MMP)-sensitive peptide were added to PEGDMA [20]. It was associated with lower COLX expression compared to PEGDMA alone showing a positive chondrogenic effect with low hypertrophic differentiation. Another study from the same group using MSCs overexpressing Nuclear Receptor subfamily 2 group F member 2 (NR2F2), which display higher chondrogenic potential than naïve MSCs, reported the formation of a neocartilage tissue after *in vivo* implantation of the 3D bioprinted scaffolds made of GRGDS- and MMP-sensitive peptides associated to PEGDA [103]. Finally, inkjet printing was also used to print a graphene oxide-supplemented COLI/chitosan hydrogel containing chondrocytes that generated *in vivo* a cartilage matrix rich in ACAN and COLI [104].

5. Light-assisted 3D bioprinting

5.1. Principle

Light-assisted 3DBP (LA3DBP) relies on two major techniques: (i) Stereolithography (SLA) and (ii) Digital Light Processing (DLP). They have in common the use of a non-polymerized bioink bath in which the printing platform is diving (Fig. 1). The platform is isolated from the bath surface in SLA (bottom-down approach) or from the bottom window in DLP (bottom-up approach) by a thin layer of bioink that will be photopolymerized. SLA uses a unique UV laser that is projected point-by-point on the bioink following the designed pattern. DLP, also known as mask-Projection Stereolithography (PSL), uses a light source that projects the pattern of the entire layer and polymerizes the bioink film at once. In both techniques, the platform then moves, up or down, to print a new layer of bioink and the process is repeated until the whole construct is printed.

5.2. Printing settings

Bioinks used in LA3DBP must be photocurable and transparent, at least in the wavelength used for photopolymerization, which is initiated by a photoinitiator. The photoinitiator present in the bioink absorbs the light and releases ROS that are responsible for the chemical reaction based on covalent bond formation. Accuracy of printing depends on the efficacy of the photoinitiator to absorb light and therefore the thickness of the light beam [55]. It also depends on the light intensity to efficaciously polymerize the bioink, as referred to as the working curve. Exposure must be set to allow the polymerizing layer to be in contact with the previously polymerized layer [105]. As such, a key property of bioinks used in LA3DBP is that they should display a Newtonian behavior (displaying a linear relationship between viscosity and shear stress) to ensure successive polymerization of the different layers. This fluid property might be associated with cell sedimentation, notably when printing large constructs but can be counterbalanced by having a smooth movement of the SLA/DLP printing platform between each polymerization step.

5.3. Advantages and limitations

The main advantage of LA3DBP is the high resolution even at high speed, both with SLA (10 µm) and DLP (25–50 µm), that allows bioprinting of porous constructs and complex shapes such as gyroids or braces, recreating the micro-architecture of cartilage tissue [6,55,106]. Resolution is strongly dependent on numerous factors: energy of the laser, printing speed, rheology and thickness of the bioink layer, shape of the 3D model, substrate wettability. In addition, LA3DBP permits to print bioinks containing high cell densities (up to 25×10^6/mL) with excellent global viability since few mechanical stresses are applied to cells [107]. It appears as a good intermediate to print bioinks that are too viscous to be inkjet-printed or not viscous enough to be extruded with great potential in mimicking the microenvironment (for review, see Ref. [108]).

The main disadvantage of this technique is the high cost of printers compared to extrusion or inkjet bioprinters. Besides, LA3DBP is not suitable to print large constructs since it requires large amounts of bioinks and cells, which are generally the limiting factors when using bioink baths. Cells printed with the LA3DBP technique are subjected to chemical stress due to ROS exposure, and to a lesser extent, to UVs. Stress can be limited by the use of compatible photoinitiator, such as Ru/SPS (tris-bipyridylruthenium(II) hexahydrate/sodium persulfate), which can efficiently absorb in visible light instead of UV [55]. Use of visible light decreases cell stress but does not reduce ROS production [106]. Nevertheless, impact of ROS can be reduced by adding an antioxidant, such as N-acetyl cysteine or catalase in the bioink, which both improve cell survival [109,110]. For these reasons, LA3DBP suffers from a lack of diversity in adapted bioinks at the moment, further limited by the choice of photoinitiator since the final mix needs to be water-soluble.

Table 2
Types of bioink used in inkjet-based bioprinting for cartilage tissue engineering applications.

Bioink base component	Other components	Crosslinking method	Polymer scaffold	Cell source	References
GELATIN					Gurkan, 2014 [76]
ALGINATE	Nanofibrillated cellulose	Ca2+	/	Chondrocytes	Markstedt, 2015 [47]
COLLAGEN	Agarose	Temperature or Fmoc-based gelation	/	HEK-293T or Chondrocytes	Graham, 2017 [45] Betsch, 2018 [46]
	Chitosan + Graphene oxide	/	/	Chondrocytes	Cheng, 2020 [87]
PEGDMA	/	UV	/	Chondrocytes	Cui, 2012 [84] Cui, 2012 [85]
	GelMA	UV	/	MSCs	Gao, 2015 [15]
	Acrylated peptides	UV	/	MSCs	Gao, 2015 [16] Gao, 2017 [86]
PEGDA	/	UV	/	MSCs	Gao, 2017 [81]

5.4. Laser-based 3DBP applied to cartilage

Laser-based bioprinting is the technique that benefits from the least improvements up to date. This is in line with few studies applied to cartilage TE (Table 3). **GelMA** is again found to be used for its biocompatibility, with high COLII and AGG expressions obtained with chondrocytes cultured for 14 days after bioprinting and **HAMA**-based bioinks induced similarly high expression levels of these ECM components [107]. In a recent study, stratified constructs with different ratios of **GelMA and HAMA** containing porcine chondrocytes were generated to mimic the zonal structure of cartilage [111]. Over 14 days, maintenance of the stratification associated with high expression of COLII and proteoglycans was observed compared to single blend constructs. Interestingly, the construct stiffness can be tuned by modulating the content of GelMA and HAMA; constructs with more HAMA having a higher Young's modulus. The addition of PEGDA to GelMA hydrogels greatly improved printing resolution while TGFβ1 embedded in nanospheres enhanced the chondrogenic differentiation of MSCs [112]. GelMA combined with decellularized ECM and MSC-derived extracellular vesicles was successfully fabricated using SLA technology and shown to facilitate cartilage repair *in vivo* [113]. **Polyvinyl alcohol (PVA)** alone or in association with GelMA revealed that GelMA was essential for long-term cell survival [55]. **Poly(DL-lactide) (PDLLA)--PEG** in association with HA allowed MSC differentiation in chondrogenic medium with elevated COLII and ACAN expression, GAGs and proteoglycan production confirming formation of cartilage ECM [106]. Interesting results were also obtained using **silk fibroin** that was methacrylated to adapt it to the technique [114]. By doing so, constructs promoting great cell viability over 14 days were obtained, with the formation of neocartilage as denoted by an increased GAG content as well as expression of cartilage-specific genes: COLII, COLX, SOX9 and ACAN at week 4. Subcutaneous implantation of the constructs in nude mice revealed production of cartilage ECM and COL matrix formation at week 8. Homogenous cell distribution within the implant was observed, which is of importance since the absence of infiltration by endogenous cells needs to be counterbalanced by a fully cellularized implant. Interesting results were also obtained using synthetic polymers.

6. Multitool and zonal approach 3D bioprinting for complex cartilaginous construct engineering

In order to add a level of complexity in the bioprinted constructs to ensure more physiological applications, some authors have developed techniques to either print multi-materials and/or different cell types and/or different cell concentrations within the same constructs. The three previously described methods can be merged to benefit from the advantages of each when combined. This can be done using some bioprinters that include multiple printheads or can receive custom-made printheads. To build stratified osteochondral implants, an interesting approach was to reinforce MSC-laden alginate hydrogels with a 3D printed polymer network made of PCL, PLA or PLGA and form biphasic cartilaginous constructs with higher potential to generate cartilage *in vivo* [115]. Another strategy was the use of FDM to pre-print PCL microchambers, allowing the subsequent deposit of MSC and chondrocyte suspensions by inkjet printing [65]. After FDM printing of the PCL framework, microextrusion was used to fill alternating pores of the PCL framework with MSC-loaded GelMA, with the aim of mimicking subchondral bone, or acellular Pluronic, which was then eluted to form channels allowing medium circulation. Finally, bioink-free chondrocyte/MSC suspensions were inkjet bioprinted on top of the chambers to let them aggregate and form a homogenous cartilaginous surface. This multitool fabrication allowed to generate a human sized tibial plateau with a collagen fibers-rich surface, which were oriented similarly to native cartilage (i.e., parallel to the top at the surface while turning perpendicular in the bottom). The large size and robustness of this construct, made possible by the PCL scaffold, allowed authors to apply cyclic mechanical stimuli, which resulted in enhanced GAG deposition compared to non-stimulated constructs. This is an interesting example of merging the previously discussed bioprinting techniques while combining more classical methods such as pellet aggregation with the aim to get closer to a structurally organized cartilage tissue.

Hybrid constructs based on inkjet printing and electrospinning can be printed to generate complex structures with controlled architecture and higher mechanical properties [116]. Alternative layers of electrospinned PCL-based fibers and jet-printed chondrocytes-laden fibrin/-collagen hydrogels can form cartilage-like tissues *in vitro* and *in vivo* that displayed enhanced mechanical properties compared to fibrin/collagen hydrogels alone.

Printing of constructs featuring a cell density, an ECM composition and gradients able to mimic the anisotropy of articular cartilage and even osteochondral regeneration has been investigated. For instance, GelMA-based bioinks have been used to improve chondrogenesis and zonal differentiation of a biphasic construct comprising of (i) a top phase made of articular cartilage-derived chondroprogenitors-laden GelMA/Gellan gum/HAMA gel to replicate the superficial zone of cartilage and (ii) a bottom phase made of MSCs-laden GelMA/Gellan gum-based gel to mimic the middle/deep zone of cartilage [117]. The biphasic construct revealed an increased content of proteoglycan 4 (PRG4) in the bottom zone of the printed construct compared to mono-composition constructs. Compared to casted biphasic constructs, lower levels of articular cartilage markers (GAGs, ACAN, COLII) and higher levels of COLI were observed. This correlated with the potential effect of the printing process on cell biological functions, notably a possible delay in matrix production compared to cells undergoing casting. The authors thus failed to obtain proper zonal differentiation of cartilage, but their study highlighted the need of better analyzing the biological consequences of the printing process, apart from viability.

Shim et al. described another interesting osteochondral application with the printing of a PCL biphasic construct with lower layers printed with an atelocollagen-based bioink embedding human MSCs and Bone Morphogenetic Protein 2 (BMP-2) covered by superior layers made of a HA-based bioink embedding MSCs and TGFβ [61]. They first confirmed the potential of such constructs *in vitro*, i.e., cytocompatibility, cell proliferation, cell morphology and differentiation in the two zones, before implanting them in rabbits with knee defects. The *in vivo* analysis showed a remarkable osteochondral regeneration at week 8 with no degeneration of the adjacent cartilage. Formation of integrated thick neocartilage tissue at the center of the osteochondral defect and

Table 3
Types of bioink used in laser-based bioprinting for cartilage tissue engineering applications.

Bioink base component	Other components	Crosslinking method	Polymer scaffold	Cell source	Reference
GELATIN	/	UV	/	Chondrocytes	Lam, 2019 [90]
	HA	UV	/	Chondrocytes	Shopperly, 2022 [111]
	PEGDA + TGFß1-containing PLGA nanospheres	UV	/	MSCs	Zhu, 2018 [94]
	ECM + Exosome	UV		MSCs	Chen, 2019 [95]
	PVA-MA	UV	/	MSCs or APCP	Lim, 2018 [50]
HYALURONIC ACID	/	UV	/	Chondrocytes	Lam, 2019 [90]
	PDLLA-PEG	UV	/	MSCs	Sun, 2015 [89]
SILK FIBROIN	/	UV	/	Chondrocytes	Hong, 2020 [96]

formation of the lacuna structure – a typical cellular morphology of cartilage – were confirmed. Moreover, they found expression of COLII and COLX throughout the articular cartilage and in the bone/cartilage interface respectively, confirming zonal cartilage regeneration. Regarding the bone layer, the authors observed new bone formation at the subchondral site but quantitative analysis is lacking, since only histological analysis was performed at this stage.

Finally, another approach chose to print COLII-based bioinks with chondrocyte density gradients to assess the formation of zonal cartilage with distinct superficial, middle and deep zones [79]. The authors used three concentrations of (i) 2×10^7 cells/mL (high cell density), (ii) 1×10^7 cells/mL (biomimetic cell density) and (iii) 0.5×10^7 cells/mL (low cell density) that they individually printed to create a gradient of high cell density in the superficial zone to low cell density in the deep zone. They showed concentrations of COLII, PRG4 and GAGs in the superficial zones regardless of the initial cell concentration, with a decreased concentration of these markers with depth. This demonstrated the possibility to print zonal cartilage with ECM production correlating cell density gradients. Nevertheless, this model presents a certain number of limitations, notably the fact that those results were obtained in static conditions while we know that articular cartilage produces specific ECM in accordance with the mechanical stimuli it receives. Besides, *in vivo* testing is necessary to confirm proper integration of the bioprinted construct in the surrounding tissues of a cartilage defect.

Altogether, these studies highlighted the interest to combine multiple printing technologies and to generate multiphasic constructs to best reproduce the complexity of native articular cartilage.

7. *In situ* printing

If most of cartilage bioprinting studies try to replicate cartilage *in vitro*, O'Connel et al. designed the Biopen, a handheld device to be surgically used to fill cartilaginous defects *in situ* [118]. Improved in further publications, the Biopen is a pen including two different cartridges, the first one being loaded with an acellular GelMA hydrogel containing a photoinitiator and the second one being loaded with GelMA embedding MSCs without photoinitiator [59,70,71]. When the operator turns on the pen, both materials are extruded, the first one forming the shell of the filament and the second one forming its core. By doing so, when the defect is filled and the filament is photopolymerized, MSCs in the inner core are protected from the UV and ROS emitted by the photoinitiator. This method has proven its superiority compared to a monoaxial extruder [59]. Robotic-assisted 3DBP approaches were also evaluated where cartilage defects are scanned for the modeling of the replacement construct through CAD and then filled by direct printing in the defect with the perfect filling shape [119]. A robotic arm was conceptualized to be theoretically able to print a construct *in situ* in a micro-invasive fashion since all its movements go through a unique point named the Remote Center of Motion. This robotic arm comprises three printheads including (i) a probe head to build the 3D model of the defect, (ii) a drilling head to excise defect margins and (iii) an extruder head to print in the defect and that can also photopolymerize the bioink.

8. Summary and perspectives

3D printing technologies have rapidly evolved and the commercialization of better suitable 3D printers has accelerated the development of 3DBP technologies that are still in the early stages of progress. The choice of the printing technology can be dictated by the rheological specifications of studied bioinks, or it can be chosen first for its advantages in terms of printing resolution or of construct volume to print that will dictate the bioink choice (Fig. 3 and Table 4). Even though LA3DBP methods look promising because of their rapidity and accuracy of printing, extrusion-based 3DBP is the most suited method to print large constructs, but it has a few technological and biological drawbacks to overcome before large scale applications in the regenerative medicine field.

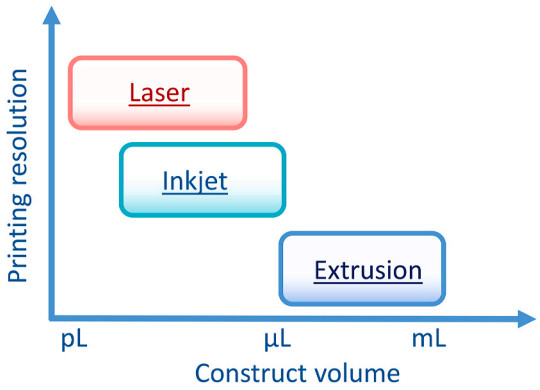

Fig. 3. Schematic summary of limits relative to printing resolution and printing volume using the three main 3DBP techniques.

Table 4
Advantages and Limitations of the different 3D Bioprinting Techniques.

	Extrusion-based Bioprinting	Inkjet Bioprinting	Light-assisted Bioprinting
Cell viability	Good (*40-80%)*	High (*>85%)*	High *85–95%)(*
Printing resolution	Moderate (*Median resolution of 400 µm)*	Excellent (*Drops as small as 30 µm)*	Excellent (*10 µm in SLA, 25-50 µm in DLP)*
Variety of bioinks available	Wide	Limited	Limited
Printing speed	Intermediate	Fast	Fast
Cell density	Intermediate (*Up to 10^8 cells/mL)*	Low (*Up to 10^7 cells/mL)*	High (*Up to $25x10^6$ cells/mL)*
Large-size construct printing	Yes	No	No
Co-printing possibility	Yes	Yes	No
Affordability	Intermediate	Cost-effective	Highly expensive

Challenges remain in the development of bioinks with improved properties for cartilage TE, including biocompatibility and chondroinductivity, mechanical stiffness, biodegradability compatible with ECM production and integration within host tissue after implantation. Printing performance of bioinks can be optimized by defining appropriate parameters for printing. One critical issue is to reduce the mechanical forces that induce shear stress on cells during printing and impact cell viability. Computational Fluid Dynamics (CFD) stimulation can help optimizing printing parameters by analyzing the material flow in the printing head. The material flow can be simulated to interconnect biomaterial properties (rheology, density), printing parameters (speed, temperature), needle geometry and length, extrusion-related mechanical forces and predict the mechanical stress applied on the cells during printing [120]. Simulation results have been validated with experimental results in a study using a cell-imprinted-based microfluidic device [121]. The study shows that parameters such as injection speed, size and number of cells, notably MSCs and chondrocytes, as well as channel dimensions can be selected to define the experimental conditions without wasting time and materials. However, most CFD studies are limited by the fact that they are specific of a bioink and nozzle characteristics [52,122]. Machine learning can also be used to validate the computational model and find out the parameters influencing the shear stress and cell viability [123].

The ultimate goal is to develop a biomimetic osteochondral tissue reproducing the complex zonal architecture of native articular cartilage in contact with the subchondral bone for optimal repair of articular osteochondral lesions. Future 3DBP strategies should therefore take into

account the possibility of including a gradient structure and the release of different growth factors to increase cartilage or bone formation and *in vivo* repair. This might be completed with the emergence of 4DBP approaches that rely on improvement of bioinks and technologies, including time-dependent changes, dynamic culture or electrostimulation. Indeed, bioinks should be responsive to different environmental stimuli. As an example, growth factors could be encapsulated within nanostructures with different release kinetics and combined with the bioink for the spatio-temporal control of cell differentiation or chondrocyte phenotype stability. Dynamic culture is of particular interest for cartilage TE since it allows compressive/tensile loads on the bioprinted constructs, which are known to increase the production of ECM components and promote the formation of cartilage [65]. Interestingly, recent studies also indicate that additional functions can be added to the bioink, which can be of particular interest for cartilage reconstruction in an inflammatory environment. Indeed, development of bioinks with innate anti-oxidant or anti-inflammatory properties have shown promising results [124,125]. Finally, the proof-of-concept has been provided that magnetism-based alignment of collagen fibers during printing or electromagnetic field exposure after printing allowed to generate constructs with increased expression of COLII [50,78]. Further development of dynamic culture within bioreactors and biophysical stimulation of constructs should therefore be envisaged for improved cartilage repair strategies.

Author contributions

All authors: writing and reviewing; Danièle Noël: writing, reviewing and editing.

Funding and acknowledgements

Authors would like to acknowledge funding support from the Inserm Institute, the University of Montpellier. We also acknowledge the Agence Nationale pour la Recherche for support of the national infrastructure: “ECELLFRANCE: Development of a national adult mesenchymal stem cell based therapy platform” (ANR-11-INSB-005). The authors acknowledge the tissue engineering facility CARTIGEN supported by the FEDER/Region Occitanie program.

Declaration of competing interest

The authors declare that they have no known competing financial interests or personal relationships that could have appeared to influence the work reported in this paper.

Data availability

No data was used for the research described in the article.

References

[1] M.B. Goldring, Update on the biology of the chondrocyte and new approaches to treating cartilage diseases, Best Pract. Res. Clin. Rheumatol. 20 (5) (2006) 1003–1025.
[2] H. Muir, The chondrocyte, architect of cartilage. Biomechanics, structure, function and molecular biology of cartilage matrix macromolecules, Bioessays 17 (12) (1995) 1039–1048.
[3] W.S. Toh, C.B. Foldager, M. Pei, J.H. Hui, Advances in mesenchymal stem cell-based strategies for cartilage repair and regeneration, Stem Cell Rev. 10 (5) (2014) 686–696.
[4] Y. Zhou, J. Chyu, M. Zumwalt, Recent progress of fabrication of cell scaffold by electrospinning technique for articular cartilage tissue engineering, Int J Biomater 2018 (2018), 1953636.
[5] H. Ding, Y. Cheng, X. Niu, Y. Hu, Application of electrospun nanofibers in bone, cartilage and osteochondral tissue engineering, J. Biomater. Sci. Polym. Ed. 32 (4) (2021) 536–561.
[6] L. Belk, N. Tellisi, H. Macdonald, A. Erdem, N. Ashammakhi, I. Pountos, Safety considerations in 3D bioprinting using mesenchymal stromal cells, Front. Bioeng. Biotechnol. 8 (2020) 924.
[7] A.R. Armiento, M.J. Stoddart, M. Alini, D. Eglin, Biomaterials for articular cartilage tissue engineering: learning from biology, Acta Biomater. 65 (2018) 1–20.
[8] E.B. Hunziker, Articular cartilage repair: basic science and clinical progress. A review of the current status and prospects, Osteoarthritis Cartilage 10 (6) (2002) 432–463.
[9] C. Bougault, L. Cueru, J. Bariller, M. Malbouyres, A. Paumier, A. Aszodi, Y. Berthier, F. Mallein-Gerin, A.M. Trunfio-Sfarghiu, Alteration of cartilage mechanical properties in absence of beta1 integrins revealed by rheometry and FRAP analyses, J. Biomech. 46 (10) (2013) 1633–1640.
[10] B.L. Wong, W.C. Bae, K.R. Gratz, R.L. Sah, Shear deformation kinematics during cartilage articulation: effect of lubrication, degeneration, and stress relaxation, Mol. Cell. BioMech. 5 (3) (2008) 197–206.
[11] M. Fortin, J. Soulhat, A. Shirazi-Adl, E.B. Hunziker, M.D. Buschmann, Unconfined compression of articular cartilage: nonlinear behavior and comparison with a fibril-reinforced biphasic model, J. Biomech. Eng. 122 (2) (2000) 189–195.
[12] P. Julkunen, W. Wilson, J.S. Jurvelin, J. Rieppo, C.J. Qu, M.J. Lammi, R. K. Korhonen, Stress-relaxation of human patellar articular cartilage in unconfined compression: prediction of mechanical response by tissue composition and structure, J. Biomech. 41 (9) (2008) 1978–1986.
[13] B. Roushangar Zineh, M.R. Shabgard, L. Roshangar, An experimental study on the mechanical and biological properties of bio-printed alginate/halloysite nanotube/methylcellulose/Russian olive-based scaffolds, Adv. Pharmaceut. Bull. 8 (4) (2018) 643–655.
[14] M. Kesti, M. Muller, J. Becher, M. Schnabelrauch, M. D'Este, D. Eglin, M. Zenobi-Wong, A versatile bioink for three-dimensional printing of cellular scaffolds based on thermally and photo-triggered tandem gelation, Acta Biomater. 11 (2015) 162–172.
[15] C.C. Lin, K.S. Anseth, PEG hydrogels for the controlled release of biomolecules in regenerative medicine, Pharm. Res. (N. Y.) 26 (3) (2009) 631–643.
[16] L. Valot, J. Martinez, A. Mehdi, G. Subra, Chemical insights into bioinks for 3D printing, Chem. Soc. Rev. 48 (15) (2019) 4049–4086.
[17] J. Crecente-Campo, E. Borrajo, A. Vidal, M. Garcia-Fuentes, New scaffolds encapsulating TGF-beta3/BMP-7 combinations driving strong chondrogenic differentiation, Eur. J. Pharm. Biopharm. 114 (2017) 69–78.
[18] S.F. Khattak, S.R. Bhatia, S.C. Roberts, Pluronic F127 as a cell encapsulation material: utilization of membrane-stabilizing agents, Tissue Eng. 11 (5–6) (2005) 974–983.
[19] G. Gao, A.F. Schilling, K. Hubbell, T. Yonezawa, D. Truong, Y. Hong, G. Dai, X. Cui, Improved properties of bone and cartilage tissue from 3D inkjet-bioprinted human mesenchymal stem cells by simultaneous deposition and photocrosslinking in PEG-GelMA, Biotechnol. Lett. 37 (11) (2015) 2349–2355.
[20] G. Gao, T. Yonezawa, K. Hubbell, G. Dai, X. Cui, Inkjet-bioprinted acrylated peptides and PEG hydrogel with human mesenchymal stem cells promote robust bone and cartilage formation with minimal printhead clogging, Biotechnol. J. 10 (10) (2015) 1568–1577.
[21] V.H. Mouser, A. Abbadessa, R. Levato, W.E. Hennink, T. Vermonden, D. Gawlitta, J. Malda, Development of a thermosensitive HAMA-containing bio-ink for the fabrication of composite cartilage repair constructs, Biofabrication 9 (1) (2017), 015026.
[22] A.X. Sun, H. Lin, M.R. Fritch, H. Shen, P.G. Alexander, M. DeHart, R.S. Tuan, Chondrogenesis of human bone marrow mesenchymal stem cells in 3-dimensional, photocrosslinked hydrogel constructs: effect of cell seeding density and material stiffness, Acta Biomater. 58 (2017) 302–311.
[23] A. Kosik-Koziol, M. Costantini, A. Mroz, J. Idaszek, M. Heljak, J. Jaroszewicz, E. Kijenska, K. Szoke, N. Frerker, A. Barbetta, J.E. Brinchmann, W. Swieszkowski, 3D bioprinted hydrogel model incorporating beta-tricalcium phosphate for calcified cartilage tissue engineering, Biofabrication 11 (3) (2019), 035016.
[24] J. Yu, S. Lee, S. Choi, K.K. Kim, B. Ryu, C.Y. Kim, C.R. Jung, B.H. Min, Y.Z. Xin, S. A. Park, W. Kim, D. Lee, J. Lee, Fabrication of a polycaprolactone/alginate bipartite hybrid scaffold for osteochondral tissue using a three-dimensional bioprinting system, Polymers 12 (10) (2020).
[25] J.P. Armstrong, M. Burke, B.M. Carter, S.A. Davis, A.W. Perriman, 3D bioprinting using a templated porous bioink, Adv Healthc Mater 5 (14) (2016) 1724–1730.
[26] T. Gonzalez-Fernandez, S. Rathan, C. Hobbs, P. Pitacco, F.E. Freeman, G. M. Cunniffe, N.J. Dunne, H.O. McCarthy, V. Nicolosi, F.J. O'Brien, D.J. Kelly, Pore-forming bioinks to enable spatio-temporally defined gene delivery in bioprinted tissues, J. Contr. Release 301 (2019) 13–27.
[27] Z. Li, X. Zhang, T. Yuan, Y. Zhang, C. Luo, J. Zhang, Y. Liu, W. Fan, Addition of platelet-rich plasma to silk fibroin hydrogel bioprinting for cartilage regeneration, Tissue Eng. 26 (15–16) (2020) 886–895.
[28] T. Moller, M. Amoroso, D. Hagg, C. Brantsing, N. Rotter, P. Apelgren, A. Lindahl, L. Kolby, P. Gatenholm, Vivo chondrogenesis in 3D bioprinted human cell-laden hydrogel constructs, Plast Reconstr Surg Glob Open 5 (2) (2017) e1227.
[29] M. Muller, E. Ozturk, O. Arlov, P. Gatenholm, M. Zenobi-Wong, Alginate sulfate-nanocellulose bioinks for cartilage bioprinting applications, Ann. Biomed. Eng. 45 (1) (2017) 210–223.
[30] S. Rathan, L. Dejob, R. Schipani, B. Haffner, M.E. Mobius, D.J. Kelly, Fiber reinforced cartilage ECM functionalized bioinks for functional cartilage tissue engineering, Adv Healthc Mater 8 (7) (2019), e1801501.
[31] L.S. Teixeira, J. Feijen, C.A. van Blitterswijk, P.J. Dijkstra, M. Karperien, Enzyme-catalyzed crosslinkable hydrogels: emerging strategies for tissue engineering, Biomaterials 33 (5) (2012) 1281–1290.
[32] X. Cui, J. Li, Y. Hartanto, M. Durham, J. Tang, H. Zhang, G. Hooper, K. Lim, T. Woodfield, Advances in extrusion 3D bioprinting: a focus on multicomponent hydrogel-based bioinks, Adv Healthc Mater 9 (15) (2020), e1901648.

[33] M. Costantini, J. Idaszek, K. Szoke, J. Jaroszewicz, M. Dentini, A. Barbetta, J. E. Brinchmann, W. Swieszkowski, 3D bioprinting of BM-MSCs-loaded ECM biomimetic hydrogels for in vitro neocartilage formation, Biofabrication 8 (3) (2016), 035002.

[34] J. Idaszek, M. Costantini, T.A. Karlsen, J. Jaroszewicz, C. Colosi, S. Testa, E. Fornetti, S. Bernardini, M. Seta, K. Kasarello, R. Wrzesien, S. Cannata, A. Barbetta, C. Gargioli, J.E. Brinchman, W. Swieszkowski, 3D bioprinting of hydrogel constructs with cell and material gradients for the regeneration of full-thickness chondral defect using a microfluidic printing head, Biofabrication 11 (4) (2019), 044101.

[35] Y. Jiang, J. Chen, C. Deng, E.J. Suuronen, Z. Zhong, Click hydrogels, microgels and nanogels: emerging platforms for drug delivery and tissue engineering, Biomaterials 35 (18) (2014) 4969–4985.

[36] C. Henrionnet, L. Pourchet, P. Neybecker, O. Messaoudi, P. Gillet, D. Loeuille, D. Mainard, C. Marquette, A. Pinzano, Combining innovative bioink and low cell density for the production of 3D-bioprinted cartilage substitutes: a pilot study, Stem Cell. Int. 2020 (2020), 2487072.

[37] Y.P. Singh, A. Bandyopadhyay, B.B. Mandal, 3D bioprinting using cross-linker-free silk-gelatin bioink for cartilage tissue engineering, ACS Appl. Mater. Interfaces 11 (37) (2019) 33684–33696.

[38] Y. Sun, Y. You, W. Jiang, Z. Zhai, K. Dai, 3D-bioprinting a genetically inspired cartilage scaffold with GDF5-conjugated BMSC-laden hydrogel and polymer for cartilage repair, Theranostics 9 (23) (2019) 6949–6961.

[39] K.Y. Lee, D.J. Mooney, Alginate: properties and biomedical applications, Prog. Polym. Sci. 37 (1) (2012) 106–126.

[40] L. Kock, C.C. van Donkelaar, K. Ito, Tissue engineering of functional articular cartilage: the current status, Cell Tissue Res. 347 (3) (2012) 613–627.

[41] E.M. Darling, K.A. Athanasiou, Rapid phenotypic changes in passaged articular chondrocyte subpopulations, J. Orthop. Res. 23 (2) (2005) 425–432.

[42] Z. Izadifar, T. Chang, W. Kulyk, X. Chen, B.F. Eames, Analyzing biological performance of 3D-printed, cell-impregnated hybrid constructs for cartilage tissue engineering, Tissue Eng. C Methods 22 (3) (2016) 173–188.

[43] J. O'Sullivan, S. D'Arcy, F.P. Barry, J.M. Murphy, C.M. Coleman, Mesenchymal chondroprogenitor cell origin and therapeutic potential, Stem Cell Res. Ther. 2 (1) (2011) 8.

[44] M. Maumus, D. Guerit, K. Toupet, C. Jorgensen, D. Noel, Mesenchymal stem cell-based therapies in regenerative medicine: applications in rheumatology, Stem Cell Res. Ther. 2 (14) (2011) 6.

[45] M.E. Bernardo, J.A. Emons, M. Karperien, A.J. Nauta, R. Willemze, H. Roelofs, S. Romeo, A. Marchini, G.A. Rappold, S. Vukicevic, F. Locatelli, W.E. Fibbe, Human mesenchymal stem cells derived from bone marrow display a better chondrogenic differentiation compared with other sources, Connect. Tissue Res. 48 (3) (2007) 132–140.

[46] F. Legendre, D. Ollitrault, T. Gomez-Leduc, M. Bouyoucef, M. Hervieu, N. Gruchy, F. Mallein-Gerin, S. Leclercq, M. Demoor, P. Galera, Enhanced chondrogenesis of bone marrow-derived stem cells by using a combinatory cell therapy strategy with BMP-2/TGF-beta1, hypoxia, and COL1A1/HtrA1 siRNAs, Sci. Rep. 7 (1) (2017) 3406.

[47] P. Tanthaisong, S. Imsoonthornruksa, A. Ngernsoungnern, P. Ngernsoungnern, M. Ketudat-Cairns, R. Parnpai, Enhanced chondrogenic differentiation of human umbilical cord wharton's jelly derived mesenchymal stem cells by GSK-3 inhibitors, PLoS One 12 (1) (2017), e0168059.

[48] C. Antich, J. de Vicente, G. Jimenez, C. Chocarro, E. Carrillo, E. Montanez, P. Galvez-Martin, J.A. Marchal, Bio-inspired hydrogel composed of hyaluronic acid and alginate as a potential bioink for 3D bioprinting of articular cartilage engineering constructs, Acta Biomater. 106 (2020) 114–123.

[49] A.D. Graham, S.N. Olof, M.J. Burke, J.P.K. Armstrong, E.A. Mikhailova, J. G. Nicholson, S.J. Box, F.G. Szele, A.W. Perriman, H. Bayley, High-resolution patterned cellular constructs by droplet-based 3D printing, Sci. Rep. 7 (1) (2017) 7004.

[50] M. Betsch, C. Cristian, Y.Y. Lin, A. Blaeser, J. Schoneberg, M. Vogt, E.M. Buhl, H. Fischer, D.F. Duarte Campos, Incorporating 4D into bioprinting: real-time magnetically directed collagen fiber alignment for generating complex multilayered tissues, Adv Healthc Mater 7 (21) (2018), e1800894.

[51] K. Markstedt, A. Mantas, I. Tournier, H. Martinez Avila, D. Hagg, P. Gatenholm, 3D bioprinting human chondrocytes with nanocellulose-alginate bioink for cartilage tissue engineering applications, Biomacromolecules 16 (5) (2015) 1489–1496.

[52] R. Chand, B.S. Muhire, S. Vijayavenkataraman, Computational fluid dynamics assessment of the effect of bioprinting parameters in extrusion bioprinting, Int J Bioprint 8 (2) (2022) 545.

[53] R. Chang, J. Nam, W. Sun, Effects of dispensing pressure and nozzle diameter on cell survival from solid freeform fabrication-based direct cell writing, Tissue Eng. 14 (1) (2008) 41–48.

[54] J.M. Baena, G. Jimenez, E. Lopez-Ruiz, C. Antich, C. Grinan-Lison, M. Peran, P. Galvez-Martin, J.A. Marchal, Volume-by-volume bioprinting of chondrocytes-alginate bioinks in high temperature thermoplastic scaffolds for cartilage regeneration, Exp. Biol. Med. 244 (1) (2019) 13–21.

[55] K.S. Lim, R. Levato, P.F. Costa, M.D. Castilho, C.R. Alcala-Orozco, K.M.A. van Dorenmalen, F.P.W. Melchels, D. Gawlitta, G.J. Hooper, J. Malda, T.B. F. Woodfield, Bio-resin for high resolution lithography-based biofabrication of complex cell-laden constructs, Biofabrication 10 (3) (2018), 034101.

[56] J.H. Galarraga, M.Y. Kwon, J.A. Burdick, 3D bioprinting via an in situ crosslinking technique towards engineering cartilage tissue, Sci. Rep. 9 (1) (2019), 19987.

[57] M. Yeo, J. Ha, H. Lee, G. Kim, Fabrication of hASCs-laden structures using extrusion-based cell printing supplemented with an electric field, Acta Biomater. 38 (2016) 33–43.

[58] B. Gatenholm, C. Lindahl, M. Brittberg, S. Simonsson, Collagen 2A type B induction after 3D bioprinting chondrocytes in situ into osteoarthritic chondral tibial lesion, Cartilage 13 (2_suppl) (2021) 1755S–1769S.

[59] S. Duchi, C. Onofrillo, C.D. O'Connell, R. Blanchard, C. Augustine, A.F. Quigley, R.M.I. Kapsa, P. Pivonka, G. Wallace, C. Di Bella, P.F.M. Choong, Handheld Co-Axial Bioprinting: application to in situ surgical cartilage repair, Sci. Rep. 7 (1) (2017) 5837.

[60] Y. Gu, L. Zhang, X. Du, Z. Fan, L. Wang, W. Sun, Y. Cheng, Y. Zhu, C. Chen, Reversible physical crosslinking strategy with optimal temperature for 3D bioprinting of human chondrocyte-laden gelatin methacryloyl bioink, J. Biomater. Appl. 33 (5) (2018) 609–618.

[61] J.H. Shim, K.M. Jang, S.K. Hahn, J.Y. Park, H. Jung, K. Oh, K.M. Park, J. Yeom, S. H. Park, S.W. Kim, J.H. Wang, K. Kim, D.W. Cho, Three-dimensional bioprinting of multilayered constructs containing human mesenchymal stromal cells for osteochondral tissue regeneration in the rabbit knee joint, Biofabrication 8 (1) (2016), 014102.

[62] S. Stichler, T. Bock, N. Paxton, S. Bertlein, R. Levato, V. Schill, W. Smolan, J. Malda, J. Tessmar, T. Blunk, J. Groll, Double printing of hyaluronic acid/poly (glycidol) hybrid hydrogels with poly(epsilon-caprolactone) for MSC chondrogenesis, Biofabrication 9 (4) (2017), 044108.

[63] S. Romanazzo, S. Vedicherla, C. Moran, D.J. Kelly, Meniscus ECM-functionalised hydrogels containing infrapatellar fat pad-derived stem cells for bioprinting of regionally defined meniscal tissue, J Tissue Eng Regen Med 12 (3) (2018) e1826–e1835.

[64] T.J. Hinton, Q. Jallerat, R.N. Palchesko, J.H. Park, M.S. Grodzicki, H.J. Shue, M. H. Ramadan, A.R. Hudson, A.W. Feinberg, Three-dimensional printing of complex biological structures by freeform reversible embedding of suspended hydrogels, Sci. Adv. 1 (9) (2015), e1500758.

[65] A.C. Daly, D.J. Kelly, Biofabrication of spatially organised tissues by directing the growth of cellular spheroids within 3D printed polymeric microchambers, Biomaterials 197 (2019) 194–206.

[66] M. Muller, J. Becher, M. Schnabelrauch, M. Zenobi-Wong, Nanostructured Pluronic hydrogels as bioinks for 3D bioprinting, Biofabrication 7 (3) (2015), 035006.

[67] N. Diamantides, C. Dugopolski, E. Blahut, S. Kennedy, L.J. Bonassar, High density cell seeding affects the rheology and printability of collagen bioinks, Biofabrication 11 (4) (2019), 045016.

[68] A. Bandyopadhyay, B.B. Mandal, N. Bhardwaj, 3D bioprinting of photo-crosslinkable silk methacrylate (SilMA)-polyethylene glycol diacrylate (PEGDA) bioink for cartilage tissue engineering, J. Biomed. Mater. Res. 110 (4) (2022) 884–898.

[69] B. Wang, P.J. Diaz-Payno, D.C. Browe, F.E. Freeman, J. Nulty, R. Burdis, D. J. Kelly, Affinity-bound growth factor within sulfated interpenetrating network bioinks for bioprinting cartilaginous tissues, Acta Biomater. 128 (2021) 130–142.

[70] C. Onofrillo, S. Duchi, C.D. O'Connell, R. Blanchard, A.J. O'Connor, M. Scott, G. G. Wallace, P.F.M. Choong, C. Di Bella, Biofabrication of human articular cartilage: a path towards the development of a clinical treatment, Biofabrication 10 (4) (2018), 045006.

[71] C. Di Bella, S. Duchi, C.D. O'Connell, R. Blanchard, C. Augustine, Z. Yue, F. Thompson, C. Richards, S. Beirne, C. Onofrillo, S.H. Bauquier, S.D. Ryan, P. Pivonka, G.G. Wallace, P.F. Choong, In Situ Handheld Three-Dimensional Bioprinting for Cartilage Regeneration, J Tissue Eng Regen Med, 2017.

[72] Z. Yang, T. Zhao, C. Gao, F. Cao, H. Li, Z. Liao, L. Fu, P. Li, W. Chen, Z. Sun, S. Jiang, Z. Tian, G. Tian, K. Zha, T. Pan, X. Li, X. Sui, Z. Yuan, S. Liu, Q. Guo, 3D-Bioprinted difunctional scaffold for in situ cartilage regeneration based on aptamer-directed cell recruitment and growth factor-enhanced cell chondrogenesis, ACS Appl. Mater. Interfaces 13 (20) (2021) 23369–23383.

[73] D. Nguyen, D.A. Hagg, A. Forsman, J. Ekholm, P. Nimkingratana, C. Brantsing, T. Kalogeropoulos, S. Zaunz, S. Concaro, M. Brittberg, A. Lindahl, P. Gatenholm, A. Enejder, S. Simonsson, Cartilage tissue engineering by the 3D bioprinting of iPS cells in a nanocellulose/alginate bioink, Sci. Rep. 7 (1) (2017) 658.

[74] M. Lafuente-Merchan, S. Ruiz-Alonso, A. Zabala, P. Galvez-Martin, J.A. Marchal, B. Vazquez-Lasa, I. Gallego, L. Saenz-Del-Burgo, J.L. Pedraz, Chondroitin and Dermatan Sulfate Bioinks for 3D Bioprinting and Cartilage Regeneration, Macromol Biosci, 2022, e2100435.

[75] P. Apelgren, M. Amoroso, K. Saljo, A. Lindahl, C. Brantsing, L. Stridh Orrhult, K. Markstedt, P. Gatenholm, L. Kolby, Long-term in vivo integrity and safety of 3D-bioprinted cartilaginous constructs, J. Biomed. Mater. Res. B Appl. Biomater. 109 (1) (2021) 126–136.

[76] X. Barcelo, K.F. Eichholz, O. Garcia, D.J. Kelly, Tuning the degradation rate of alginate-based bioinks for bioprinting functional cartilage tissue, Biomedicines 10 (7) (2022).

[77] Y. Chu, L. Huang, W. Hao, T. Zhao, H. Zhao, W. Yang, X. Xie, L. Qian, Y. Chen, J. Dai, Long-term stability, high strength, and 3D printable alginate hydrogel for cartilage tissue engineering application, Biomed. Mater. 16 (6) (2021).

[78] H.G. Yi, K.S. Kang, J.M. Hong, J. Jang, M.N. Park, Y.H. Jeong, D.W. Cho, Effects of electromagnetic field frequencies on chondrocytes in 3D cell-printed composite constructs, J. Biomed. Mater. Res. 104 (7) (2016) 1797–1804.

[79] X. Ren, F. Wang, C. Chen, X. Gong, L. Yin, L. Yang, Engineering zonal cartilage through bioprinting collagen type II hydrogel constructs with biomimetic chondrocyte density gradient, BMC Muscoskel. Disord. 17 (2016) 301.

[80] X. Yang, Z. Lu, H. Wu, W. Li, L. Zheng, J. Zhao, Collagen-alginate as bioink for three-dimensional (3D) cell printing based cartilage tissue engineering, Mater Sci Eng C Mater Biol Appl 83 (2018) 195–201.

[81] J. Hauptstein, L. Forster, A. Nadernezhad, J. Groll, J. Tessmar, T. Blunk, Tethered TGF-beta1 in a hyaluronic acid-based bioink for bioprinting cartilaginous tissues, Int. J. Mol. Sci. 23 (2) (2022).

[82] S. Nedunchezian, P. Banerjee, C.Y. Lee, S.S. Lee, C.W. Lin, C.W. Wu, S.C. Wu, J. K. Chang, C.K. Wang, Generating adipose stem cell-laden hyaluronic acid-based scaffolds using 3D bioprinting via the double crosslinked strategy for chondrogenesis, Mater Sci Eng C Mater Biol Appl 124 (2021), 112072.

[83] J. Hauptstein, L. Forster, A. Nadernezhad, H. Horder, P. Stahlhut, J. Groll, T. Blunk, J. Tessmar, Bioink platform utilizing dual-stage crosslinking of hyaluronic acid tailored for chondrogenic differentiation of mesenchymal stromal cells, Macromol. Biosci. 22 (2) (2022), e2100331.

[84] S.W. Kim, D.Y. Kim, H.H. Roh, H.S. Kim, J.W. Lee, K.Y. Lee, Three-dimensional bioprinting of cell-laden constructs using polysaccharide-based self-healing hydrogels, Biomacromolecules 20 (5) (2019) 1860–1866.

[85] A. Scalzone, G. Cerqueni, M.A. Bonifacio, M. Pistillo, S. Cometa, M.M. Belmonte, X.N. Wang, K. Dalgarno, A.M. Ferreira, E. De Giglio, P. Gentile, Valuable effect of Manuka Honey in increasing the printability and chondrogenic potential of a naturally derived bioink, Mater Today Bio 14 (2022), 100287.

[86] X. Zhang, Y. Liu, C. Luo, C. Zhai, Z. Li, Y. Zhang, T. Yuan, S. Dong, J. Zhang, W. Fan, Crosslinker-free silk/decellularized extracellular matrix porous bioink for 3D bioprinting-based cartilage tissue engineering, Mater Sci Eng C Mater Biol Appl 118 (2021), 111388.

[87] F. Pati, J. Jang, D.H. Ha, S. Won Kim, J.W. Rhie, J.H. Shim, D.H. Kim, D.W. Cho, Printing three-dimensional tissue analogues with decellularized extracellular matrix bioink, Nat. Commun. 5 (2014) 3935.

[88] K. Behan, A. Dufour, O. Garcia, D. Kelly, Methacrylated cartilage ECM-based hydrogels as injectables and bioinks for cartilage tissue engineering, Biomolecules 12 (2) (2022).

[89] E.V. Isaeva, E.E. Beketov, G.A. Demyashkin, N.D. Yakovleva, N.V. Arguchinskaya, A.A. Kisel, T.S. Lagoda, E.P. Malakhov, A.N. Smirnova, V.M. Petriev, P.S. Eremin, E.O. Osidak, S.P. Domogatsky, S.A. Ivanov, P.V. Shegay, A.D. Kaprin, Cartilage Formation in vivo using high concentration collagen-based bioink with MSC and decellularized ECM granules, Int. J. Mol. Sci. 23 (5) (2022).

[90] Y.S. Kim, M. Majid, A.J. Melchiorri, A.G. Mikos, Applications of decellularized extracellular matrix in bone and cartilage tissue engineering, Bioeng Transl Med 4 (1) (2019) 83–95.

[91] S.V. Murphy, A. Atala, 3D bioprinting of tissues and organs, Nat. Biotechnol. 32 (8) (2014) 773–785.

[92] A. Faulkner-Jones, S. Greenhough, J.A. King, J. Gardner, A. Courtney, W. Shu, Development of a valve-based cell printer for the formation of human embryonic stem cell spheroid aggregates, Biofabrication 5 (1) (2013), 015013.

[93] U.A. Gurkan, R. El Assal, S.E. Yildiz, Y. Sung, A.J. Trachtenberg, W.P. Kuo, U. Demirci, Engineering anisotropic biomimetic fibrocartilage microenvironment by bioprinting mesenchymal stem cells in nanoliter gel droplets, Mol. Pharm. 11 (7) (2014) 2151–2159.

[94] J. de Jong, G. de bruin, H. Reinten, M. van den Berg, H. Wijshoff, M. Versluis, D. Lohse, Air entrapment in piezo-driven inkjet printheads, J. Acoust. Soc. Am. 120 (3) (2006) 1257–1265.

[95] R.E. Saunders, J.E. Gough, B. Derby, Delivery of human fibroblast cells by piezoelectric drop-on-demand inkjet printing, Biomaterials 29 (2) (2008) 193–203.

[96] B. He, S. Yang, Z. Qin, B. Wen, C. Zhang, The roles of wettability and surface tension in droplet formation during inkjet printing, Sci. Rep. 7 (1) (2017), 11841.

[97] F.-G. Tseng, C.-J. Kim, C.-M. Ho, A high-resolution high-frequency monolithic top-shooting microinjector free of satellite drops - part II: fabrication, implementation, and characterization, JMEMS 11 (5) (2002) 437–447.

[98] G. Gao, K. Hubbell, A.F. Schilling, G. Dai, X. Cui, Bioprinting cartilage tissue from mesenchymal stem cells and PEG hydrogel, Methods Mol. Biol. 1612 (2017) 391–398.

[99] X. Cui, D. Dean, Z.M. Ruggeri, T. Boland, Cell damage evaluation of thermal inkjet printed Chinese hamster ovary cells, Biotechnol. Bioeng. 106 (6) (2010) 963–969.

[100] C. Li, A. Faulkner-Jones, A.R. Dun, J. Jin, P. Chen, Y. Xing, Z. Yang, Z. Li, W. Shu, D. Liu, R.R. Duncan, Rapid formation of a supramolecular polypeptide-DNA hydrogel for in situ three-dimensional multilayer bioprinting, Angew Chem. Int. Ed. Engl. 54 (13) (2015) 3957–3961.

[101] X. Cui, K. Breitenkamp, M.G. Finn, M. Lotz, D.D. D'Lima, Direct human cartilage repair using three-dimensional bioprinting technology, Tissue Eng. 18 (11–12) (2012) 1304–1312.

[102] X. Cui, K. Breitenkamp, M. Lotz, D. D'Lima, Synergistic action of fibroblast growth factor-2 and transforming growth factor-beta1 enhances bioprinted human neocartilage formation, Biotechnol. Bioeng. 109 (9) (2012) 2357–2368.

[103] G. Gao, X.F. Zhang, K. Hubbell, X. Cui, NR2F2 regulates chondrogenesis of human mesenchymal stem cells in bioprinted cartilage, Biotechnol. Bioeng. 114 (1) (2017) 208–216.

[104] Z. Cheng, L. Xigong, D. Weiyi, H. Jingen, W. Shuo, L. Xiangjin, W. Junsong, Potential use of 3D-printed graphene oxide scaffold for construction of the cartilage layer, J. Nanobiotechnol. 18 (1) (2020) 97.

[105] B. van Bochove, G. Hannink, P. Buma, D.W. Grijpma, Preparation of designed poly(trimethylene carbonate) meniscus implants by stereolithography: challenges in stereolithography, Macromol. Biosci. 16 (12) (2016) 1853–1863.

[106] A.X. Sun, H. Lin, A.M. Beck, E.J. Kilroy, R.S. Tuan, Projection stereolithographic fabrication of human adipose stem cell-incorporated biodegradable scaffolds for cartilage tissue engineering, Front. Bioeng. Biotechnol. 3 (2015) 115.

[107] T. Lam, T. Dehne, J.P. Kruger, S. Hondke, M. Endres, A. Thomas, R. Lauster, M. Sittinger, L. Kloke, Photopolymerizable gelatin and hyaluronic acid for stereolithographic 3D bioprinting of tissue-engineered cartilage, J. Biomed. Mater. Res. B Appl. Biomater. 107 (8) (2019) 2649–2657.

[108] C. Mandrycky, Z. Wang, K. Kim, D.H. Kim, 3D bioprinting for engineering complex tissues, Biotechnol. Adv. 34 (4) (2016) 422–434.

[109] S. Datta, A. Das, A.R. Chowdhury, P. Datta, Bioink formulations to ameliorate bioprinting-induced loss of cellular viability, Biointerphases 14 (5) (2019), 051006.

[110] G. Rijal, B.S. Kim, F. Pati, D.H. Ha, S.W. Kim, D.W. Cho, Robust tissue growth and angiogenesis in large-sized scaffold by reducing H2O2-mediated oxidative stress, Biofabrication 9 (1) (2017), 015013.

[111] L.K. Shopperly, J. Spinnen, J.P. Kruger, M. Endres, M. Sittinger, T. Lam, L. Kloke, T. Dehne, Blends of gelatin and hyaluronic acid stratified by stereolithographic bioprinting approximate cartilaginous matrix gradients, J. Biomed. Mater. Res. B Appl. Biomater. 110 (10) (2022) 2310–2322.

[112] W. Zhu, H. Cui, B. Boualam, F. Masood, E. Flynn, R.D. Rao, Z.Y. Zhang, L. G. Zhang, 3D bioprinting mesenchymal stem cell-laden construct with core-shell nanospheres for cartilage tissue engineering, Nanotechnology 29 (18) (2018), 185101.

[113] P. Chen, L. Zheng, Y. Wang, M. Tao, Z. Xie, C. Xia, C. Gu, J. Chen, P. Qiu, S. Mei, L. Ning, Y. Shi, C. Fang, S. Fan, X. Lin, Desktop-stereolithography 3D printing of a radially oriented extracellular matrix/mesenchymal stem cell exosome bioink for osteochondral defect regeneration, Theranostics 9 (9) (2019) 2439–2459.

[114] H. Hong, Y.B. Seo, D.Y. Kim, J.S. Lee, Y.J. Lee, H. Lee, O. Ajiteru, M.T. Sultan, O. J. Lee, S.H. Kim, C.H. Park, Digital light processing 3D printed silk fibroin hydrogel for cartilage tissue engineering, Biomaterials 232 (2020), 119679.

[115] S. Critchley, E.J. Sheehy, G. Cunniffe, P. Diaz-Payno, S.F. Carroll, O. Jeon, E. Alsberg, P.A.J. Brama, D.J. Kelly, 3D printing of fibre-reinforced cartilaginous templates for the regeneration of osteochondral defects, Acta Biomater. 113 (2020) 130–143.

[116] T. Xu, K.W. Binder, M.Z. Albanna, D. Dice, W. Zhao, J.J. Yoo, A. Atala, Hybrid printing of mechanically and biologically improved constructs for cartilage tissue engineering applications, Biofabrication 5 (1) (2013), 015001.

[117] V.H.M. Mouser, R. Levato, A. Mensinga, W.J.A. Dhert, D. Gawlitta, J. Malda, Bio-ink development for three-dimensional bioprinting of hetero-cellular cartilage constructs, Connect. Tissue Res. 61 (2) (2020) 137–151.

[118] C.D. O'Connell, C. Di Bella, F. Thompson, C. Augustine, S. Beirne, R. Cornock, C. J. Richards, J. Chung, S. Gambhir, Z. Yue, J. Bourke, B. Zhang, A. Taylor, A. Quigley, R. Kapsa, P. Choong, G.G. Wallace, Development of the Biopen: a handheld device for surgical printing of adipose stem cells at a chondral wound site, Biofabrication 8 (1) (2016), 015019.

[119] J. Lipskas, K. Deep, W. Yao, Robotic-assisted 3D bio-printing for repairing bone and cartilage defects through a minimally invasive approach, Sci. Rep. 9 (1) (2019) 3746.

[120] J. Emmermacher, D. Spura, J. Cziommer, D. Kilian, T. Wollborn, U. Fritsching, J. Steingroewer, T. Walther, M. Gelinsky, A. Lode, Engineering considerations on extrusion-based bioprinting: interactions of material behavior, mechanical forces and cells in the printing needle, Biofabrication 12 (2) (2020), 025022.

[121] S. Yazdian Kashani, M. Keshavarz Moraveji, S. Bonakdar, Computational and experimental studies of a cell-imprinted-based integrated microfluidic device for biomedical applications, Sci. Rep. 11 (1) (2021), 12130.

[122] J. Gohl, K. Markstedt, A. Mark, K. Hakansson, P. Gatenholm, F. Edelvik, Simulations of 3D bioprinting: predicting bioprintability of nanofibrillar inks, Biofabrication 10 (3) (2018), 034105.

[123] E. Reina-Romo, S. Mandal, P. Amorim, V. Bloemen, E. Ferraris, L. Geris, Towards the experimentally-informed in silico nozzle design optimization for extrusion-based bioprinting of shear-thinning hydrogels, Front. Bioeng. Biotechnol. 9 (2021), 701778.

[124] Y. Huang, X. Meng, Z. Zhou, W. Zhu, X. Chen, Y. He, N. He, X. Han, D. Zhou, X. Duan, P.M. Vadgama, H. Liu, A naringin-derived bioink enhances the shape fidelity of 3D bioprinting and efficiency of cartilage defect repair, J. Mater. Chem. B 10 (36) (2022) 7030–7044.

[125] W. Shi, F. Fang, Y. Kong, S.E. Greer, M. Kuss, B. Liu, W. Xue, X. Jiang, P. Lovell, A. M. Mohs, A.T. Dudley, T. Li, B. Duan, Dynamic hyaluronic acid hydrogel with covalent linked gelatin as an anti-oxidative bioink for cartilage tissue engineering, Biofabrication 14 (1) (2021).